reduced the amounts of Dlg1 and Scribble in the soluble fraction, they increased those in the insoluble fraction (Fig. 3). Since Tax1 or its mutants had little effect on the amount of Dlg1 and Scribble in the total lysates, these results indicated that Tax1 changes the subcellular localization of Scribble as well as Dlg1 from the detergent soluble fraction into the insoluble one. In addition, Tax1 induced a slower-migrating form of Dlg1 in the insoluble and total fraction (lanes 7–10 in Fig. 3). This is likely to be due to the phosphorylation of Dlg1 described previously [25].

To further establish the interaction of Dlg1 and Scribble with the Tax1 mutants, their subcellular localizations in the absence or presence of Tax1 were examined by immunostaining. In 293T cells, endogenous Dlg1 and Scribble was localized primarily at the plasma membrane (Fig. 4). The transiently transduced Tax1 was localized in the nucleus and in the cytoplasm, and some were colocalized with Dlg1 and Scribble at the perinuclear region as large granules that were not observed without Tax1. Tax1ΔC was localized in the nucleus and in the cytoplasm and formed large granules at the perinuclear regions similar to that observed in Tax1, but these granules contained neither Dlg1 nor Scribble. These results suggested that Tax1 was colocalized with endogenous Dlg1 and Scribble in a PBM-dependent manner. Similar to Tax1, M2 was also colocalized with Dlg1 and Scribble at the perinuclear regions as large granules. On the other hand, the colocalization of M1 only with Dlg1, but not Scribble, was detected, and the colocalization of M3 neither with Dlg1 nor Scribble were detected. Since M1 and M3 as well as Tax1 interacted with both endogenous Dlg1 and Scribble in an immunoprecipitation assay (Fig. 2), these results may therefore indicate that M1 and M3 transiently interact with Dlg1 and Scribble; however, the amounts of which remains at undetectable levels based on an immunostaining assay.

To examine the effect of Tax1 on the localization of Dlg1 and Scribble in HTLV-1-infected T-cell lines, cell lysates were prepared from the indicated T-cell lines. Consistently with the transient transfection of Tax1 into 293T cells, HTLV-1-infected T-cell lines (MT-4, SLB-1) showed a reduced amount of Dlg1 and Scribble in the soluble fraction and an increased amount in the insoluble fraction in comparison to HTLV-1-uninfected T-cell lines (Jurkat, MOLT-4; Fig. 5). These results suggested that Tax1 in HTLV-1-infected T-cell lines is likely to induce the translocation of Dlg1 and Scribble from the detergent soluble fraction into the insoluble one.

Discussion

Subgroups of HTLV, HPV, and human adenovirus have oncoproteins with PBM, and the motif is associated with their oncogenic potentials in vivo. However, whether one motif has substitutable function(s) with the other PBMs has not been clarified. The present study showed that two different PBMs from HPV-16 E6 and E4ORF1 of human adenovirus type 9 can substitute the function of Tax1 PBM

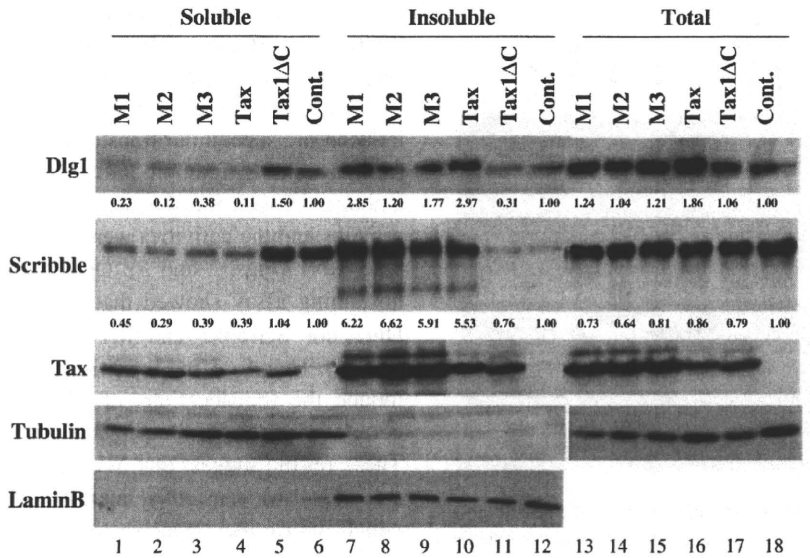

Fig. 3 Tax1 PBM mutants induce the subcellular translocation of Dlg1 and Scribble. Soluble, insoluble and total cell lysates were prepared from 293T cells transfected with the expression plasmids encoding the indicated Tax1 mutant or the control plasmid (*Cont*) as described in the Materials and methods. The lysates were characterized by a Western blotting analysis using anti-Dlg1, anti-Scribble, or anti-Tax1 antibody. The intensities of the respective bands were measured by a densitometer (Gel-Doc; Bio-Rad), and the numbers beneath the bands were calculated as a ratio of the intensity of the band in question relative to that of the Control (*Cont*)

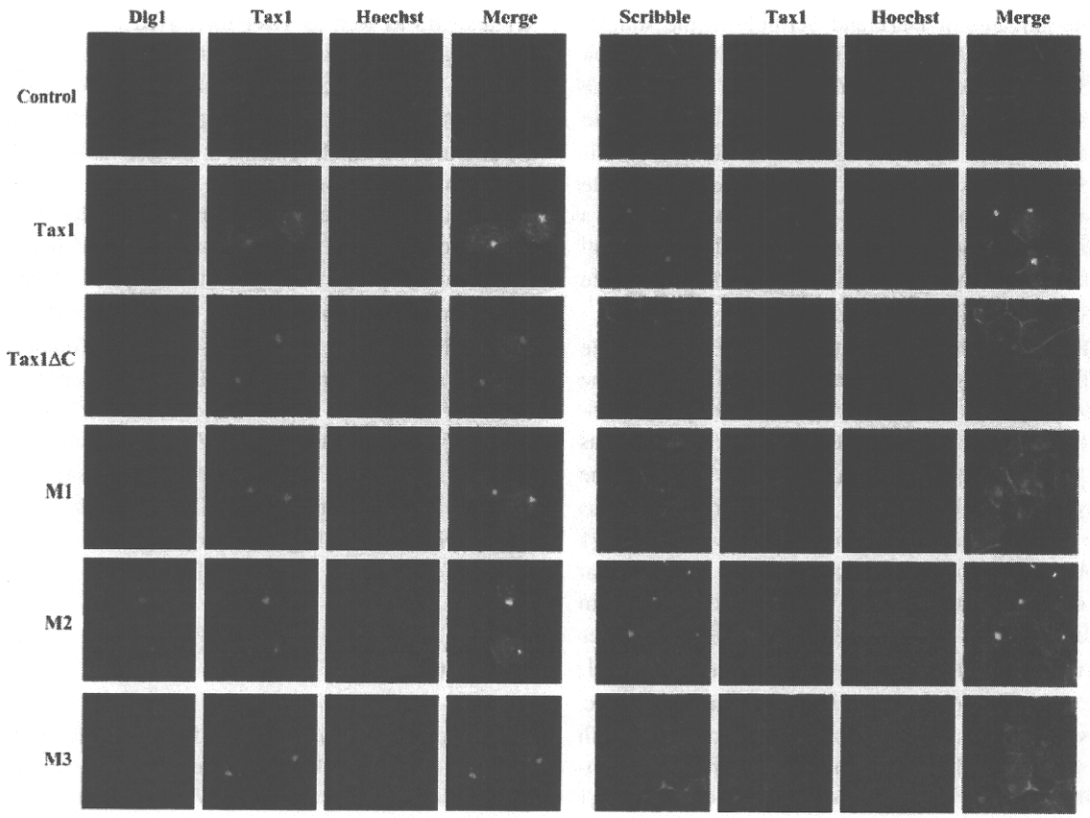

Fig. 4 Colocalization of Tax1 with Dlg1 and Scribble. 293T cells were transfected with either the pHβPr-neo-Tax1, pHβPr-neo-Tax1ΔC, pHβPr-neo-Tax1M1, pHβPr-neo-Tax1M2 or pHβPr-neo-Tax1M3 plasmid using the lipofection method. At 48 h after transfection, the cells were fixed and were stained with anti-Tax1 and with Hoechst 33258 together either with anti-Dlg1 or anti-Scribble. The stained cells were examined using fluorescent light microscopy

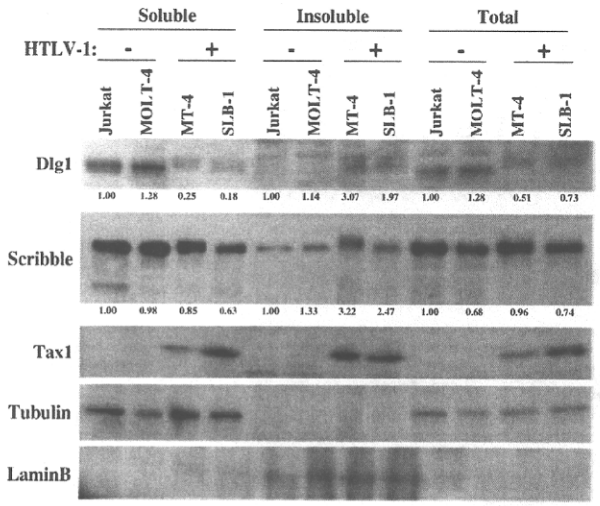

Fig. 5 Expression of Dlg1 and Scribble in human T-cell lines. Soluble, insoluble and total cell lysates were prepared from the indicated human T-cell lines as described in Materials and methods. The lysates were characterized by a Western blot analysis using anti-Dlg1, anti-Scribble, or anti-Tax1 antibody. HTLV-1 infection to the cell lines was indicated. The intensities of the respective bands were measured by a densitometer (Gel-Doc; Bio-Rad), and the numbers beneath the bands were calculated as a ratio of the intensity of the band in question relative to that of Jurkat

in the transformation toward a T-cell line. Therefore, these results suggest that the motif has common function(s) in the transforming activities, thus indicating that they may play a role in the subtype-specific oncogenesis.

Three Tax1 PBM mutants, through direct interaction, induced the subcellular translocation of Dlg1 and Scribble from a soluble fraction into an insoluble one, and the amounts of such translocation were more than half of the proteins and the activities were equivalent to those of wild type Tax1 (Figs. 2 and 3). On the other hand, an immunostaining assay showed that M3 interacted neither with Dlg1 nor Scribble, and M1 only interacted with Dlg1 (Fig. 4). Therefore, the activities of Tax1 and its mutants to induce the translocations of Dlg1 and Scribble did not correlate with their colocalizations with Dlg1 and Scribble. These results suggest that M1 and M3 (and possibly Tax1 and M2 also) transiently interact with Dlg1 and Scribble, which induce their translocations, although a further analysis is required to establish this hypothesis.

M3, a Tax1 PBM mutant, has an extra seven amino acid residues relative to wild type Tax1, derived from E6 (Fig. 1a); nevertheless, the transforming activity of M3 was equivalent to that of Tax1. This result was unexpected,

since the Tax1 C-terminal amino acid residues close to the PBM are well conserved among HTLV-1 isolates but it is dissimilar to E6. Therefore, these results indicated that the PBM is structurally and functionally independent from the other part of Tax1.

While E6 induces the degradation of Dlg1 and Scribble in a PDZ-dependent manner [21], Tax1 did not or minimally induce the degradation of Dlg1 and Scribble in 293T cells, and instead it altered the subcellular localization of Dlg1 and Scribble from the soluble fraction into the insoluble fraction (Fig. 3). This is consistent with the previous study that Tax1 induces the translocation of Dlg1 from the soluble fraction into the insoluble fraction [19]. Therefore, both Tax1 and E6 are thought to inactivate these tumor-suppressor PDZ domain proteins [25], but the mechanisms may be distinct from each other. Interestingly, two Tax1 mutants with E6 PBM also did not (or minimally) induce the degradation of Dlg1 and Scribble. As a result, the region(s) of E6, other than PBM, is thus considered to be a main determinant for inducing the degradation of Dlg1 and Scribble probably by means of binding to a ubiquitin ligase, namely, E6-AP [27]. Attempts to compare the activities of Tax1 and E6 to Dlg1 and Scribble in cells were unsuccessful, since expression of E6 from the expression plasmid in 293T cells was much lower than that of Tax1 (data not shown). Thus, a further analysis is required to establish the mechanisms of Tax1 and E6 to inactivate these PDZ domain proteins.

Acknowledgments We would like to thank Dr. Hiroyuki Miyoshi at RIKEN Tsukuba Institute for providing the lentivirus plasmids. We also wish to thank the Takeda Pharmaceutical Company for providing recombinant human IL-2. We would like to express our gratitude to Misako Tobimatsu for her excellent technical assistance. This work was supported in part by a Grant-in-Aid for Scientific Research on Priority Areas and for Scientific Research (C) of Japan, as well as a Grant for the Promotion of Niigata University Research Projects.

References

1. Y. Hinuma, K. Nagata, M. Hanaoka, M. Nakai, T. Matsumoto, K.I. Kinoshita, S. Shirakawa, I. Miyoshi, Proc. Natl. Acad. Sci. USA **78**(10), 6476–6480 (1981)
2. T. Uchiyama, Annu. Rev. Immunol. **15**, 15–37 (1997)
3. R.C. Gallo, Retrovirology **2**(1), 17 (2005)
4. G. Feuer, P.L. Green, Oncogene **24**(39), 5996–6004 (2005)
5. K. Endo, A. Hirata, K. Iwai, M. Sakurai, M. Fukushi, M. Oie, M. Higuchi, W.W. Hall, F. Gejyo, M. Fujii, J. Virol. **76**(6), 2648–2653 (2002)
6. C. Tsubata, M. Higuchi, M. Takahashi, M. Oie, Y. Tanaka, F. Gejyo, M. Fujii, Retrovirology **2**, 46 (2005)
7. W.W. Hall, M. Fujii, Oncogene **24**(39), 5965–5975 (2005)
8. M. Higuchi, C. Tsubata, R. Kondo, S. Yoshida, M. Takahashi, M. Oie, Y. Tanaka, R. Mahieux, M. Matsuoka, M. Fujii, J. Virol. **81**(21), 11900–11907 (2007)
9. R. Grassmann, S. Berchtold, I. Radant, M. Alt, B. Fleckenstein, J.G. Sodroski, W.A. Haseltine, U. Ramstedt, J. Virol. **66**(7), 4570–4575 (1992)
10. T. Akagi, K. Shimotohno, J. Virol. **67**(3), 1211–1217 (1993)
11. T.M. Ross, S.M. Pettiford, P.L. Green, J. Virol. **70**(8), 5194–5202 (1996)
12. C.Z. Giam, K.T. Jeang, Front. Biosci. **12**, 1496–1507 (2007)
13. S.L. Cross, M.B. Feinberg, J.B. Wolf, N.J. Holbrook, F. Wong-Staal, W.J. Leonard, Cell **49**(1), 47–56 (1987)
14. M. Maruyama, H. Shibuya, H. Harada, M. Hatakeyama, M. Seiki, T. Fujita, J. Inoue, M. Yoshida, T. Taniguchi, Cell **48**(2), 343–350 (1987)
15. M. Fujii, H. Tsuchiya, T. Chuhjo, T. Akizawa, M. Seiki, Genes Dev. **6**(11), 2066–2076 (1992)
16. L.J. Zhao, C.Z. Giam, Proc. Natl. Acad. Sci. USA **89**(15), 7070–7074 (1992)
17. T. Suzuki, T. Narita, M. Uchida-Toita, M. Yoshida, Virology **259**(2), 384–391 (1999)
18. K. Iwai, N. Mori, M. Oie, N. Yamamoto, M. Fujii, Virology **279**(1), 38–46 (2001)
19. A. Hirata, M. Higuchi, A. Niinuma, M. Ohashi, M. Fukushi, M. Oie, T. Akiyama, Y. Tanaka, F. Gejyo, M. Fujii, Virology **318**(1), 327–336 (2004)
20. S.S. Lee, R.S. Weiss, R.T. Javier, Proc. Natl. Acad. Sci. USA **94**(13), 6670–6675 (1997)
21. R.T. Javier, Oncogene **27**(55), 7031–7046 (2008)
22. K. Ishioka, M. Higuchi, M. Takahashi, S. Yoshida, M. Oie, Y. Tanaka, S. Takahashi, L. Xie, P.L. Green, M. Fujii, Retrovirology **3**, 71 (2006)
23. Y. Tanaka, A. Yoshida, H. Tozawa, H. Shida, H. Nyunoya, K. Shimotohno, Int. J. Cancer **48**(4), 623–630 (1991)
24. M. Okajima, M. Takahashi, M. Higuchi, T. Ohsawa, S. Yoshida, Y. Yoshida, M. Oie, Y. Tanaka, F. Gejyo, M. Fujii, Virus Genes **37**(2), 231–240 (2008)
25. T. Suzuki, Y. Ohsugi, M. Uchida-Toita, T. Akiyama, M. Yoshida, Oncogene **18**(44), 5967–5972 (1999)
26. C. Arpin-Andre, J.M. Mesnard, J. Biol. Chem. **282**(45), 33132–33141 (2007)
27. Y. Matsumoto, S. Nakagawa, T. Yano, S. Takizawa, K. Nagasaka, K. Nakagawa, T. Minaguchi, O. Wada, H. Ooishi, K. Matsumoto, T. Yasugi, T. Kanda, J.M. Huibregtse, Y. Taketani, J. Med. Virol. **78**(4), 501–507 (2006)

Biomedical Research 31 (3) 199-206, 2010

Expression of a chemokine BRAK/CXCL14 in oral floor carcinoma cells reduces the settlement rate of the cells and suppresses their proliferation *in vivo*

Shin Ito[1, 2], Shigeyuki Ozawa[1, 2, 3], Takeharu Ikoma[1, 2], Nobuyuki Yajima[1, 2], Tohru Kiyono[4], and Ryu-Ichiro Hata[1, 2]

[1] Oral Health Science Research Center, [2] Department of Biochemistry and Molecular Biology, [3] Department of Oral and Maxillofacial Surgery, Kanagawa Dental College, 82 Inaoka-cho, Yokosuka, 238-8580, and [4] Virology Division, National Cancer Center Research Institute, Tokyo, 104-0045, Japan

(Received 23 March 2010; and accepted 12 May 2010)

ABSTRACT

We reported previously that the forced expression of the chemokine BRAK/CXCL14 in head and neck squamous cell carcinoma cells decreased the rate of tumor formation and size of tumor xenografts in athymic nude mice and SCID mice. In order to clarify the expression of BRAK/CXCL14 affected either the settlement of carcinoma cells in host tissues *in vivo* or proliferation of the colonized carcinoma cells or both, we prepared oral floor carcinoma-derived HSC-2 cells in which BRAK/CXCL14 expression was induced upon doxycycline treatment. Then 30 nude mice were separated into 3 groups composed of 10 mice per group: Group I, the control, in which the engineered cells were directly xenografted onto the back of the mice; Group II, the cells were xenografted and then the mice were treated with doxycycline; and Group III, the cells were pretreated with doxycycline during culture, and the host mice were also treated with the drug before and after xenografting. The effects of BRAK/CXCL14 expression were examined by measuring the tumor size. The order of the size of tumor xenografts was Group I > II > III, even though the growth rate of the engineered cells was the same whether or not the cells were cultured in the presence of the drug. In addition, the size of tumors was significantly down-regulated after xenografting the doxycycline-pretreated cells in Group III. These data indicate that BRAK/CXCL14 expression in oral floor carcinoma cells reduced both the rate of settlement and the proliferation of the cells *in vivo* after settlement of the cells.

Chemokines are a family of small (8–14 kDa) mostly basic, structurally related chemotactic cytokines, and they function as leukocyte subtype-selective chemo-attractants (29, 30). A complex network of chemokines and their receptors influences the development of primary tumors and metastasis (2, 19, 29).

First detected in breast and kidney, BRAK is also called CXC chemokine ligand 14 (CXCL14), and was reported to induce B cell, monocyte (26), and dendritic cell infiltration into normal and tumour tissues (25) and to inhibit angiogenesis (23). Generally, BRAK/CXCL14 is expressed universally and abundantly in normal tissues but is absent from or expressed only in a very small amount in cancerous tissues *in vivo* and in carcinoma cells in culture, including head and neck squamous cell carcinoma (HNSCC) cells (7, 9, 11, 16, 23). On the other hand, heightened BRAK/CXCL14 expression has been reported to occur in adenocarcinomas such as prostate (22), breast cancer (1) and pancreatic cancer cells (28). These data suggest that the effects of BRAK/CXCL14 on the development and progression of cancer might be quite different between HN-

Address correspondence to: Dr. Ryu-Ichiro Hata, Oral Health Science Research Center, Kanagawa Dental College, 82 Inaoka-cho, Yokosuka, 238-8580, Japan
Tel: +81-46-822-9587, Fax: +81-46-822-9587
E-mail: ryuhata@gmail.com

SCC and adenocarcinoma.

We reported previously that the forced expression of BRAK/CXCL14 in tongue carcinoma cells decreased the rate of tumor formation and size of tumor xenografts in athymic nude mice (16) and SCID mice (17). In these experiments on cloned cells with an upregulated BRAK/CXCL14 protein expression, the growth of these cells under culture conditions was the same as that of control mock vector-transfected cells. However, the migration rate of the BRAK/CXCL14-expressing cells *in vitro* was significantly slower than that of the mock-vector transfected cells and attachment of the cells to collagen was much faster than the control cells (21).

Recent progress in cancer research has shown that cancerous tissues *in vivo* are derived from colonies of cancer stem cells (3, 10, 14, 18). These data raised 3 possibilities regarding the apparent slower growth rate of xenografted BRAK/CXCL14-expressing tumor cells. The first is that the ratio of stem cell-like cells among the BRAK/CXCL14-expressing cells was smaller, and thus a smaller number of carcinoma cells settled in the tissues of the host mice. The second possibility is that the growth rate of BRAK/CXCL14-expressing cells *in vivo* was slower than that of mock-vector transfected cells. The third one is that both the rate of settlement and proliferation of the cells *in vivo* after settlement of the cells was reduced.

In order to assess either BRAK/CXCL14 expression in tumor cells regulates settlement of tumor cells in the tissue or proliferation of the colonized tumour cells or both, we employed doxycycline-inducible HSC-2 cells, which express a high amount of BRAK/CXCL14 proteins only in the presence of doxycycline (8), a derivative of tetracycline (24), referred to Tet-on BRAK HSC-2 cells.

MATERIALS AND METHODS

Materials. Dulbecco's modified Eagle's medium was obtained from Sigma (Tokyo, Japan), and gentamicin sulfate, Trypsin 250 and sucrose were from Wako Pure Chemical Industries (Osaka, Japan). Mg^{2+}-Ca^{2+}-free phosphate-buffered saline tablets PBS (−) and doxycycline were purchased from TAKARA BIO (Shiga, Japan). Fungizone came from Invitrogen (Carlsbad, CA, USA); and fetal bovine serum (FBS) from Thermo Electron (Melbourne, Australia). TetraColor ONE reagent for determination of cell proliferation was from Seikagaku Corporation (Tokyo, Japan).

Construction of Tet-on BRAK vector and preparation of Tet-on BRAK HSC-2 cells. CSII-TRE-Tight-RfA was generated by replacing the EF1a promoter in CSII-EF-RfA (a gift from Dr. H. Miyoshi, RIKEN) with a tetracycline-inducible promoter, TRE-Tight, from pTRE-Tight (Clontech). Lentiviral vector plasmid, CSII-TRE-Tight-EGFP was constructed by recombination using the Gateway system (Invitrogen) as described previously (18). The HS4 chromatin insulator from the chicken β-globin locus control region (4) was inserted into the BspE1 site in the 3'-LTR of CSII-TRE-Tight-EGFP to generate CSII(ins)-TRE-Tight-EGFP. CSII(ins)-TRE-Tight-DEST was constructed by recombination between CSII(ins)-TRE-Tight-EGFP and pDONR221. BRAK cDNA was amplified by PCR and first recombined into pDONR221 and then recombined into CSII(ins)-TRE-Tight-DEST to generate CSII(ins)-TRE-Tight-BRAK.

The recombinant lentiviruses with the vesicular stomatitis virus G glycoprotein were produced as described previously (12). Production of recombinant retroviruses was described elsewhere (13). HSC-2 cells were infected with PQCXIN-TetON retroviruses and selected in the presence of G418 (800 μg/mL). The Tet-on HSC-2 cells were then infected with CSII(ins)-TRE-Tight-BRAK or enhanced green fluorescent protein (EGFP) expressing lentiviruses at the multiplicity of infection of more than 5 so as to generate Tet-on BRAK- and Tet-on EGFP-HSC-2 cells, respectively.

Cells and cell culture. HSC-2 cells derived from an oral floor carcinoma were obtained from the Japanese Collection of Research Bioresources (JCRB). The cells were cultured in Dulbecco's modified Eagle's medium containing gentamicin sulfate (50 mg/L), Fungizone (250 mg/L) and 10% FBS in the absence or the presence of various concentrations of doxycycline. The cells were cultured at 37°C under 95% air and 5% CO_2 and routinely passaged by treatment with 0.25% trypsin/1 mM ethylenediaminetetraacetic acid in PBS (−). The growth rate of the cells was determined by TetraColor ONE assay or by measuring the number of cells with a Coulter ZI Counter (Coulter Electronics Ltd., England).

Western blot analysis. We determined BRAK/CXCL14 and β-actin protein levels by using Western blotting as previously reported (16). Cells were lysed with Laemmli buffer consisting of 62.5 mM Tris-HCl (pH 6.8) containing 2% SDS, 8% glycerol,

0.05% bromophenol blue and 5% 2-mercaptoethanol. The proteins were separated by electrophoresis in an SDS-15–20% polyacrylamide gel (SuperSep; Wako Pure Chemical Industries, Osaka, Japan) and transferred onto an Immobilon-P membrane at a constant voltage of 50 volts for 2 h. After blocked with Odyssey Blocking Buffer (LI-COR Biosciences, Lincoln, NE), the membrane was incubated for 1 h at room temperature with appropriate primary antibodies in TBS solution [20 mM Tris-HCl (pH 7.6) containing 137 mM NaCl and 0.05% Tween-20]. It was then incubated with horseradish peroxidase (HRP)-conjugated sheep anti-mouse IgG, as the secondary antibody, for 30 min at room temperature. Immunoreactive bands were visualized using Lumi-Light Western Blotting Substrate (Roche Diagnostics, Tokyo, Japan). Intensity of signals on the Western blot was calculated by Image Quant 5.1 (GE Healthcare, Tokyo, Japan).

Tumor growth in vivo. Cells (1×10^7 cells/site) were injected subcutaneously into female BALB/c nu/nu mice (specific pathogen-free; Clea Japan, Tokyo, Japan). The mice were kept under a 12-h light/ 12-h dark cycle and provided water containing 2-mg/mL doxycycline and 5% (w/v) sucrose or 5% sucrose solution only for control mice (24). Tumor volume was calculated according to the following formula: $(a \times b^2)/2$, where "a" is the longer and "b" is the shorter dimension (16). All animal experiments in this study complied with the Guidelines of the Care and Use of Laboratory Animals of Kanagawa Dental College.

Immunohistochemical procedures. Tumor xenografts were removed from the mice and embedded in O.C.T compound (Tissue-Tek; Miles Inc., Elkhart, IN) and kept at −80°C. The frozen tissues were sectioned with a cryostat at 6 μm and the air-dried sections were incubated with rat anti-CD31antibody (ER-MP12; BMA Biomedicals, Switzerland, 1 : 800 dilution) as the 1st antibody and then with biotinylated rabbit anti-rat IgG (Vector Laboratories, Inc., Burlingame, CA; 1 : 250 dilution) as the 2nd antibody. Other sections were incubated with rabbit anti-α smooth muscle actin antibody (E184; Epitomics, Inc., Burlingame, CA; 1 : 100 dilution) as the 1st antibody followed by HRP-linked donkey anti-rabbit IgG (GE Healthcare, England; 1 : 50 dilution) as the 2nd antibody. For some sections the 1st antibody was omitted and used for a negative control. Histochemical color development was achieved by Vectastatin DAB (3,3'-diaminobenzidine) substrate kit (Vector Laboratories, Inc. Burlingame, CA) according to the manufacturer's instructions, as described previously (27). Areas positively stained with anti-CD31 or anti-α smooth muscle actin antibodies were measured in 5 randomly chosen visual fields at ×200 magnification by use of a Biozero microscope (KEYENCE, Tokyo, Japan) and VH analyzer software (KEYENCE).

Statistical analysis. Student's *t*-test was used to assess statistically significant differences between 2 groups *in vitro* cell growth and *in vivo* tumor volumes with $P < 0.05$ being considered statistically significant. The Smirnov-Grubbs test was also used to determine statistically significant differences in the size of xenografted tumors.

RESULTS

Production and characterization of Tet-on BRAK HSC-2 cells

We first tried to produce doxycycline-inducible BRAK-expressing cells by using a commercially available two-step system that employs transfection reagents; however, we could not obtain cells expressing BRAK/CXCL14 protein at a high enough level to be detected by Western blotting. Thus we prepared doxycycline-inducible BRAK-expressing cells using retrovirus- and lentivirus-mediated gene transfer. Tet-on BRAK HSC-2 cells obtained here expressed BRAK/CXCL14 in both time- and doxycycline dose-dependent manners; and over a 10 times higher level of BRAK protein was expressed after 24 h of treatment with 0.1 μg/mL of doxycycline than obtained without the drug (Fig. 1A and B). In addition 100% of the cells expressed EGFP as observed under a fluorescence microscope when Tet-on EGFP HSC-2 cells were cultured in the presence of doxycycline (data not shown).

The addition of various amounts of doxycycline to the culture medium of parental HSC-2 cells did not affect the growth rate of the cells (Fig. 2A). Furthermore, the growth rate of Tet-on BRAK HSC-2 cells was not affected by the presence of 0.1 μg/mL doxycycline up-to 8 days (Doxy; Fig. 2B), at which time the cells expressed 14 times more BRAK/CXCL14 than the control (see Fig. 1B), indicating that the presence of exogenously added doxycycline or the expression of over a 10 times higher level of BRAK/CXCL14 proteins by the cells did not affect the growth of the tumor cells under the culture conditions used.

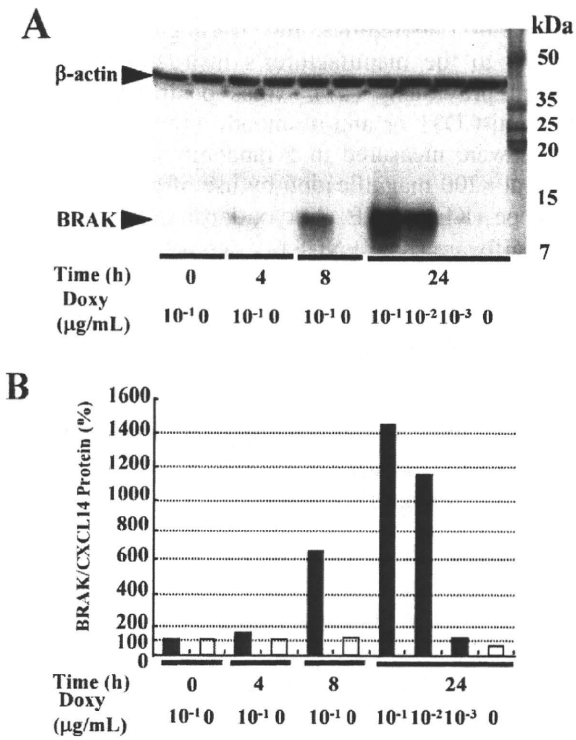

Fig. 1 Time- and doxycycline dose-dependent expression of BRAK/CXCL14 protein in Tet-on BRAK HSC-2 cells *in vitro*. The cells were cultured in the presence or absence of various concentrations of doxycycline (Doxy). (A) Proteins in the whole-cell lysates were separated by electrophoresis in SDS/15–20% polyacrylamide gels. BRAK/CXCL14 and β-actin proteins were visualized by performing Western blotting using respective antibodies. (B) The amounts of protein were determined by densitometry of the membrane shown in "A". Open columns indicate the cells cultured in the absence of doxycycline; and closed columns, those cultured in the presence of the drug.

Effects of expression of BRAK protein by Tet-on BRAK HSC-2 cells in vivo

In order to examine the effect of BRAK expression on the growth of HSC-2 cells *in vivo*, we injected Tet-on BRAK HSC-2 cells subcutaneously into mice. After 13 days, when the average size of tumors had reached 200 mm^3, we changed the drinking water from 5% sucrose solution [Group I: Doxy (−, −)] to 2 mg/mL doxycycline-containing 5% sucrose solution [Group II: Doxy (−, +)]. The growth of tumors was significantly slower in the doxycycline-treated mice than in the control animals (Fig. 3A), and tumors obtained from the former expressed a significantly higher amount of BRAK protein, as observed by Western blotting (Fig. 3B). When Tet-on BRAK HSC-2 cells were precultured for 7 days in the presence of 0.1 μg/mL of doxycycline before being injected into doxycycline-treated animals, the sizes of tumors at 6 days were significantly smaller than those at 3 days after the injection [Fig. 3A, Group III Doxy (+, +), see bracketed value], indicating that BRAK/CXCL14 expression affected the settlement of tumor cells. The sizes of tumors of Group III were always smaller than those of the tumors of doxycycline non-treated animals (Fig. 3A, Group I) and also those of animals treated with the drug after tumor cell injection (Fig. 3A, Group II). Also, the expression level of BRAK/CXCL14 protein in the tumors from the doxycycline-treated animals was significantly higher than that of controls at 34 days after transplantation (Fig. 3B). These finding thus indicate that BRAK/CXCL14 expression affected both the settlement of tumor cells and proliferation of the colonized cells.

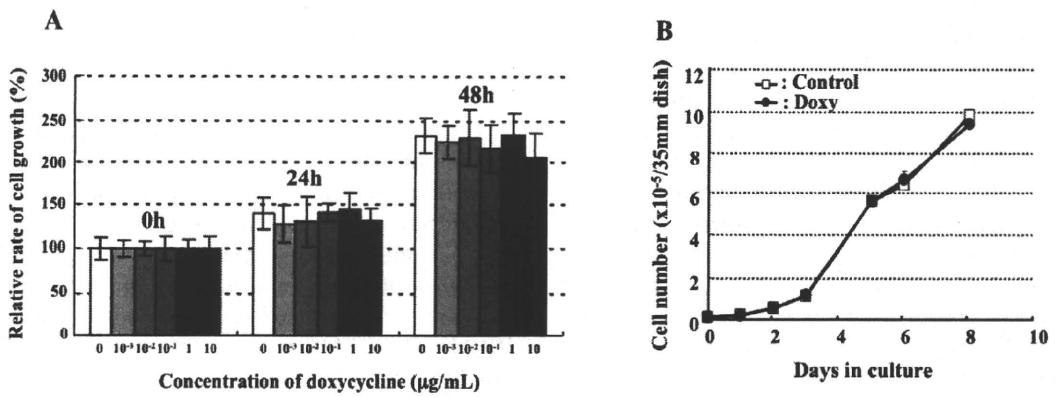

Fig. 2 Effect of doxycycline on the growth of cells. (A) HSC-2 cells (5×10^3/well) were plated on well bottom of a 96-well plate and cultured in the absence or presence of various concentrations of doxycycline for 0 to 48 h. The numbers of cells was determined by use of TetraColor One reagent. (B) Tet-on BRAK HSC-2 cells (2×10^4/35 mm dish) were plated and cultured for 8 days in the absence (open squares) or presence (closed circles) of doxycycline (0.1 μg/mL) and the number of cells was determined with a Coulter Counter.

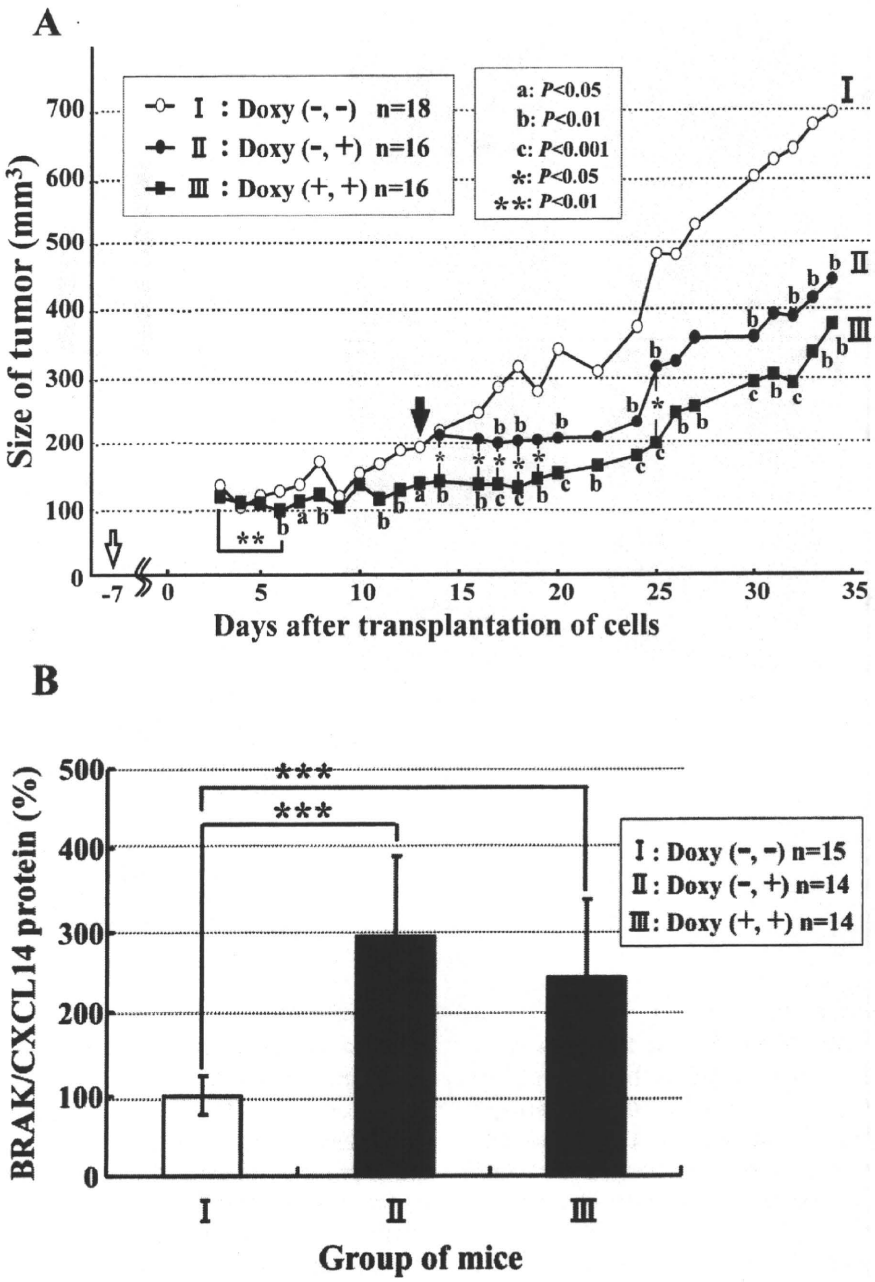

Fig. 3 Expression of BRAK/CXCL14 protein in tumor cells suppressed growth of the cells *in vivo*.
(A) Tumor size of xenografted Tet-on BRAK HSC-2 cells. The mice were subcutaneously injected with 10^7 Tet-on BRAK HSC-2 cells, and the animals were provided 5% sucrose-containing water (Group I). Other mice were given sucrose solution containing 2 mg/mL doxycycline starting at 13 days (black arrow) after implantation of the tumor cells (Group II). A third group of mice were implanted with Tet-on BRAK HSC-2 cells that had been precultured in the presence of 0.1 μg/mL of doxycycline for 7 days (Group III). These mice were provided doxycycline-supplemented water 7 days before (white arrow) implantation of the tumor cells. a, $P < 0.05$; b, $P < 0.01$; and c, $P < 0.001$ between group I and II or III. *, $P < 0.05$ between group II and III and **, $P < 0.01$ between day 3 and day 6 of group III.
(B) Expression levels of BRAK/CXCL14 proteins in transplanted tumor cells *in vivo* 35 days after transplantation, as determined by Western blotting. ***, $P < 0.001$, as indicated by the bracket.

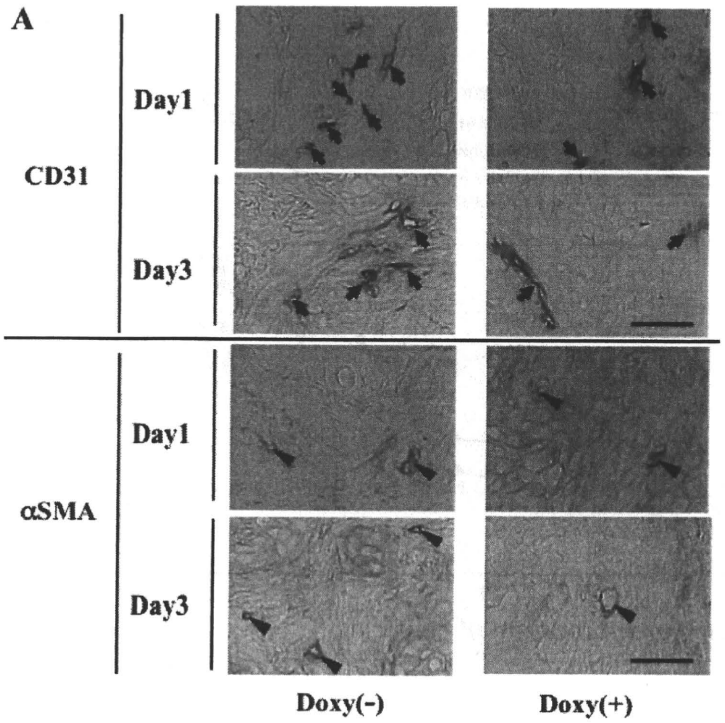

Fig. 4 Immunohistochemically stained tumor xenografts from control (Doxy –) and doxycycline treated (Doxy +) mice. (A) Frozen tumor tissue sections were stained with anti-CD31 (endothelial cell marker) antibody or anti-*α* smooth muscle actin (smooth muscle cell marker, *α*SMA) antibody. Large vascular structures were prominent in tumor xenografts from doxycycline non-treated animals. Arrows indicate endothelial cells positive for CD31 and arrowheads indicate vascular vessels positive for *α* smooth muscle actin. Bars indicate 100 μm. (B) Areas positively stained with anti-CD31 or anti-*α* smooth muscle actin (*α*SMA) were measured on 5 randomly chosen visual fields at 200 times magnifications. *: $P < 0.05$ as indicated by the bracket.

Immunohistochemical studies

In order to clarify the reason for the suppression of the tumor growth in the BRA/CXCL14-expressing cells under the *in vivo*, but not under the *in vitro* situation, we examined the infiltration of blood vessels into the tumor tissue. When vascular endothelial cells in the tumor were immunohistochemically stained with anti-CD31 antibody, the number of CD31-positive endothelial cells at 1 day and 3 days after the xenografting was the same whether or not the tumor-bearing mice had been treated with doxycycline (Fig. 4A and B). However, when the sections were stained with anti-α smooth muscle actin antibody, a marker for smooth muscle cells, the area of positive staining surrounding the endothelial cells was significantly smaller in tumors 3 days after treatment with doxycycline (Fig. 4A and B).

DISCUSSION

In HNSCC cells, including HSC-2 cells, the expression of BRAK/CXCL14 is down-regulated. The expression is negatively regulated by the binding of epidermal growth factor (EGF) to its receptor (16); and when HNSCC cells are treated with gefitinib, an epidermal growth factor tyrosine kinase inhibitor, the expression of BRAK/CXCL14 protein increases under culture conditions (15). Interestingly, the oral administration of gefitinib significantly ($P < 0.001$) reduces the growth of tumor xenografts of 3 HNSCC cell lines (HSC-2, HSC-3 and HSC-4) in female athymic nude mice, which reduction is accompanied by an increase in BRAK expression specifically in the tumor tissue; this tumor-suppressing effect of the drug is not observed in the case of BRAK non-expressing cells (15). Furthermore, the introduction of a vector expressing short hairpin RNA against BRAK reduces both the expression level of BRAK/CXCL14 in HSC-3 cells and the antitumor efficacy of gefitinib *in vivo* (15). These data indicate an inverse relationship between BRAK expression levels in tumor cells and the tumor growth

rate.

Here we showed that the expression of BRAK/CXCL14 protein induced in tumor cells by treatment with doxycycline *in vivo* resulted in significant reduction in the size of tumors compared with the size of the control mice (Fig. 3A and B), even though expression of the protein under culture conditions did not affect the rate of growth of the cells (Fig. 2A and B). The results obtained here indicate that the expression of BRAK/CXCL14 itself without the co-presence of gefitinib is sufficient to reduce the growth rate of tumors *in vivo*.

The present data showed significant down-regulation of the size of tumors shortly after tumor-cell xenografting when doxycycline-pretreated tumor cells were used and the host mice had been also pretreated with the drug before tumor cell xenografting. These results indicate that tumor cell settlement in the host tissues was also suppressed by the expression of BRAK/CXCL14 in the tumor cells.

In order to investigate further the effect of BRAK/CXCL14 expression on tumor formation, we stained the tumor tissues in the xenografted mice with anti-CD31 antibody, a marker for vascular endothelial cells. We could not find any significant difference between doxycycline-treated and un-treated animals in terms of staining intensity (Fig. 4A and B). However, a significant difference in the area positive for α smooth muscle actin was observed between tumors of doxycycline-treated and un-treated animals 3 days after injection of tumors (Fig. 4A and B). It is reported that recombinant BRAK/CXCL14 inhibits *in vivo* angiogenesis induced by IL-8 (CXCL8), basic FGF or VEGF and that binding of BRAK/CXCL14 to human umbilical vein endothelial cells and human dermal micro-vascular endothelial cells is not detectable (23). Recently it was clarified that tumor blood vessels are atypical and immature, and they have poorly developed vessel walls that are invested inadequately with vascular smooth muscle cells (4, 10). Our data coincide well with these reports and suggest the possibility that the target cell of BRAK/CXCL14 is the smooth muscle cell and not the vascular endothelial cell and that BRAK/CXCL14 inhibits the proliferation and/or chemotaxis-directed movement of smooth muscle cells, which is essential for maturation of blood vessels. Thus, such inhibition would restrain the formation of functional vessels and consequently inhibit growth of tumors.

In conclusion we showed, using Tet-on BRAK HSC-2 cells that expressed BRAK/CXCL14 protein under regulation of doxycycline, inhibition of both the settlement and proliferation of tumor cells *in vivo*, even though expression of the chemokine did not affect growth properties of the tumor cells *in vitro*. Furthermore, the suppression of the tumor growth *in vivo* was found to be at least dependent on the inhibition of maturation of tumor blood vessels. Our present findings may be useful for the clarification of the molecular mechanisms of BRAK/CXCL14 functions *in vivo*.

Acknowledgements

We thank Dr. H. Miyoshi (RIKEN) for providing lentivirus vectors and packaging constructs. We also appreciate Dr. Yasumasa Kato for valuable discussion and Ms. Etsuko Shimada for preparation of the reference list. A part of this work was performed at the Oral Health Science Research Center, Kanagawa Dental College and supported by a Grant-in Aid from the High-Tech Research Center Project of the Ministry of Education, Culture, Sports, Science and Technology of Japan (S.I., S.O, and R.H.) and by Scientific Research, Japan Society for Promotion of Sciences (R.H.). Another part of the work was performed at National Cancer Center Research Institute and supported by a Grant-in-Aid from the Ministry of Health, Labor and Welfare of Japan (T.K.).

REFERENCES

1. Allinen M, Beroukhim R, Cai L, Brennan C, Lahti-Domenici J, Huang H, Porter D, Hu M, Chin L, Richardson A, Schnitt S, Sellers WR and Polyak K (2004) Molecular characterization of the tumor microenvironment in breast cancer. *Cancer Cell* **6**, 17–32.
2. Balkwill F (2004) Cancer and the chemokine network. *Nat Rev Cancer* **4**, 540–550.
3. Castellanos A, Vicente-Duenas C, Campos-Sanchez E, Cruz JJ, Garcia-Criado FJ, Garcia-Cenador MB, Lazo PA, Perez-Losada J and Sanchez-Garcia I (2010) Cancer as a reprogramming-like disease: Implications in tumor development and treatment. *Semin Cancer Biol*, Feb 24 [Epub ahead of print].
4. Dudley AC, Khan ZA, Shih SC, Kang SY, Zwaans BM, Bischoff J and Klagsbrun M (2008) Calcification of multipotent prostate tumor endothelium. *Cancer Cell* **14**, 201–211.
5. Emery DW, Yannaki E, Tubb J and Stamatoyannopoulos G (2000) A chromatin insulator protects retrovirus vectors from chromosomal position effects. *Proc Natl Acad Sci USA* **97**, 9150–9155.
6. Frederick MJ, Henderson Y, Xu X, Deavers MT, Sahin AA, Wu H, Lewis DE, El-Naggar AK and Clayman GL (2000) In vivo expression of the novel CXC chemokine BRAK in normal and cancerous human tissue. *Am J Pathol* **156**, 1937–1950.
7. Hossini AM, Eberle J, Fecker LF, Orfanos CE and Geilen CC (2003) Conditional expression of exogenous Bcl-X(S)

triggers apoptosis in human melanoma cells in vitro and delays growth of melanoma xenografts. *FEBS Lett* **553**, 250–256.
8. Hromas R, Broxmeyer HE, Kim C, Nakshatri H, Christopherson K, 2nd, Azam M and Hou YH (1999) Cloning of BRAK, a novel divergent CXC chemokine preferentially expressed in normal versus malignant cells. *Biochem Biophys Res Commun* **255**, 703–706.
9. Koch U, Krause M and Baumann M (2010) Cancer stem cells at the crossroads of current cancer therapy failures-radiation oncology perspective. *Semin Cancer Biol*, Feb 26 [Epub ahead of print].
10. McKeage MJ and Baguley BC (2010) Disrupting established tumor blood vessels: an emerging therapeutic strategy for cancer. *Cancer* **116**, 1859–1871.
11. McKinnon CM, Lygoe KA, Skelton L, Mitter R and Mellor H (2008) The atypical Rho GTPase RhoBTB2 is required for expression of the chemokine CXCL14 in normal and cancerous epithelial cells. *Oncogene* **27**, 6856–6865.
12. Miyoshi H (2004) Gene delivery to hematopoietic stem cells using lentiviral vectors. *Methods Mol Biol* **246**, 429–438.
13. Naviaux RK, Costanzi E, Haas M and Verma I MV (1996) The pCL vector system: rapid production of helper-free, high-titer, recombinant retroviruses. *J Virol* **70**, 5701–5705.
14. O'Brien CA, Pollett A, Gallinger S and Dick JE (2007) A human colon cancer cell capable of initiating tumour growth in immunodeficient mice. *Nature* **445**, 106–110.
15. Ozawa S, Kato Y, Ito S, Komori R, Shiiki N, Tsukinoki K, Ozono S, Maehata Y, Taguchi T, Imagawa-Ishiguro Y, Tsukuda M, Kubota E and Hata RI (2009) Restoration of BRAK/CXCL14 gene expression by gefitinib is associated with antitumor efficacy of the drug in head and neck squamous cell carcinoma. *Cancer Sci* **100**, 2202–2209.
16. Ozawa S, Kato Y, Komori R, Maehata Y, Kubota E and Hata R (2006) BRAK/CXCL14 expression suppresses tumor growth *in vivo* in human oral carcinoma cells. *Biochem Biophys Res Commun* **348**, 406–412.
17. Ozawa S, Kato Y, Kubota E and Hata R (2009) BRAK/CXCL14 expression in oral carcinoma cells completely suppresses tumor cell xenografts in SCID mouse. *Biomed Res* **30**, 315–318.
18. Ricci-Vitiani L, Lombardi DG, Pilozzi E, Biffoni M, Todaro M, Peschle C and De Maria R (2007) Identification and expansion of human colon-cancer-initiating cells. *Nature* **445**, 111–115.
19. Rollins BJ (2006) Inflammatory chemokines in cancer growth and progression. *Eur J Cancer* **42**, 760–767.
20. Sasaki R, Narisawa-Saito M, Yugawa T, Fujita M, Tashiro H, Katabuchi H, and Kiyono T (2009) Oncogenic transformation of human ovarian surface epithelial cells with defined cellular oncogenes. *Carcinogenesis* **30**, 423–431.
21. Sato K, Ozawa S, Izukuri K, Kato Y and Hata RI (2010) Expression of tumor-suppressing chemokine BRAK/CXCL14 reduces cell migration rate of HSC-3 tongue carcinoma cells and stimulates attachment to collagen and formation of elongated focal adhesions in vitro. *Cell Biol Int*, **34**, 513–522.
22. Schwarze SR, Luo J, Isaacs WB and Jarrard DF (2005) Modulation of CXCL14 (BRAK) expression in prostate cancer. *Prostate* **64**, 67–74.
23. Shellenberger TD, Wang M, Gujrati M, Jayakumar A, Strieter RM, Burdick MD, Ioannides CG, Efferson CL, El-Naggar AK, Roberts D, Clayman GL and Frederick MJ (2004) BRAK/CXCL14 is a potent inhibitor of angiogenesis and a chemotactic factor for immature dendritic cells. *Cancer Res* **64**, 8262–8270.
24. Shockett P, Difilippantonio M, Hellman N and Schatz DG (1995) A modified tetracycline-regulated system provides autoregulatory, inducible gene expression in cultured cells and transgenic mice. *Proc Natl Acad Sci USA* **92**, 6522–6526.
25. Shurin GV, Ferris RL, Tourkova IL, Perez L, Lokshin A, Balkir L, Collins B, Chatta GS and Shurin MR (2005) Loss of new chemokine CXCL14 in tumor tissue is associated with low infiltration by dendritic cells (DC), while restoration of human CXCL14 expression in tumor cells causes attraction of DC both in vitro and in vivo. *J Immunol* **174**, 5490–5498.
26. Sleeman MA, Fraser JK, Murison JG, Kelly SL, Prestidge RL, Palmer DJ, Watson JD and Kumble KD (2000) B cell- and monocyte-activating chemokine (BMAC), a novel non-ELR α-chemokine. *Int Immunol* **12**, 677–689.
27. Suzuki K, Oida T, Hamada H, Hitotsumatsu O, Watanabe M, Hibi T, Yamamoto H, Kubota E, Kaminogawa S and Ishikawa H (2000) Gut cryptopatches: Direct evidence of extrathymic anatomical sites for intestinal T lymphopoiesis. *Immunity* **13**, 691–702.
28. Wente MN, Mayer C, Gaida MM, Michalski CW, Giese T, Bergmann F, Giese NA, Büchler MW and Friess H (2008) CXCL14 expression and potential function in pancreatic cancer. *Cancer Lett* **259**, 209–217.
29. Zlotnik A (2006) Chemokines and cancer. *Int J Cancer* **119**, 2026–2029.
30. Zlotnik A and Yoshie O (2000) Chemokines: a new classification system and their role in immunity. *Immunity* **12**, 121–127.

Cancer Science
The official journal of the Japanese Cancer Association

Prevalence of human papillomavirus 16/18/33 infection and p53 mutation in lung adenocarcinoma

Reika Iwakawa,[1] Takashi Kohno,[1] Masato Enari,[1] Tohru Kiyono[2] and Jun Yokota[1,3]

Divisions of [1]Biology and [2]Virology, National Cancer Center Research Institute, Tokyo, Japan

(Received March 11, 2010/Revised April 28, 2010/Accepted April 30, 2010/Accepted manuscript online May 19, 2010/Article first published online June 14, 2010)

Human papillomavirus (HPV) infection is a causative event for the development of uterine cervical carcinoma. Human papillomavirus (HPV) 16, 18, and 33 DNA has been also detected frequently in lung adenocarcinomas (AdCs) in East Asian countries; however, its prevalence in Japan remains unclear. We therefore screened for HPV 16/18/33 DNA in 297 lung AdCs in a Japanese population by multiplex PCR with type-specific primers. As reported previously, HPV 16 DNA was detected in two cervical cancer cell lines, CaSki and SiHa, while HPV 18 DNA was detected in HeLa cells, and 0.1–1.0 copies of HPV-DNA per cell were detectable by this method. However, with this method, none of the 297 lung AdCs showed positive signals for HPV 16/18/33 DNA, indicating that HPV-DNA is not or is very rarely integrated in lung AdC genomes in the Japanese. Furthermore, none of the lung AdCs showed positive signals by nested PCR with HPV 16/18 type-specific primers. Therefore, we further attempted to detect HPV 16/18/33 DNA in 91 lung cancer cell lines, including 40 AdC cell lines. Among them, 30 have been established in Japan and the remaining 61 in the USA. No HPV signals were obtained in any of the 91 cell lines by either multiplex or nested PCR, while the *p53* gene was mutated in 81 of them including 35 of the 40 AdC cell lines. These results indicate that HPV 16/18/33 infection does not play a major role in the development of lung AdC in Japan nor in the USA. (*Cancer Sci* 2010; 101: 1891–1896)

Infection with human papillomavirus (HPV) is a critical event for the development of uterine cervical cancer.[1] E6 protein, encoded by HPV, binds the host cellular tumor suppressor protein p53, and triggers its degradation through the ubiquitin pathway.[2,3] Therefore, the biological significance of continuous p53 degradation by HPV-E6 protein in cervical carcinoma is thought to be equivalent to that of p53 inactivation by genetic alterations in various other types of cancers in human carcinogenesis. The *p53* gene is frequently inactivated in lung adenocarcinoma (AdC) by mutations and/or deletions of both alleles, and the prevalence of p53 mutations in lung AdC is approximately 50% with a higher incidence in smokers.[4,5] However, p53 is not genetically altered in the other half of lung AdCs. Therefore, it is possible that p53 is inactivated by other mechanisms in lung AdC cells without p53 mutations. For this reason, there have been many reports investigating the involvement of HPV in lung AdC development. However, the prevalence of HPV infection in lung AdCs varies drastically among the reports.[5–7] Recently, reasons for a wide variation in the prevalence of HPV infection in lung cancer were investigated by two systematic surveys of a large number of publications.[6,7] A higher prevalence in Asia than in Europe was pointed out by these two investigations,[6,7] and a higher prevalence in studies using HPV type-specific primers than in those using consensus HPV primers was also pointed out in the latter investigation.[7] In East Asia (Supplementary Table S1), a high incidence of HPV infection in lung AdC was reported from Taiwan (92.8%), China (46.9%), and Korea (55.1%).[8–10] In particular, a high prevalence of HPV 16 and 18 infections was reported from Taiwan and China and of HPV 33 infection from Korea. In Japan, the incidence of HPV infection (0–19.4%) has been reported to be not as high as in other East Asian countries, but is still high enough to consider its involvement in lung AdC development.[11–14]

Taiwan, China, and Korea are geographically close to Japan and the people in these countries are ethnically also close to the Japanese. Therefore, in this study, we aimed to elucidate whether or not HPV 16, 18, and 33 are also involved in the development of lung AdC in Japan, as in Taiwan, China, and Korea. We applied a multiplex PCR method as well as a nested PCR method using type-specific primers for detection of HPV 16, 18, and 33 DNA in 275 primary and 22 metastatic lung AdCs in Japanese, and also in 91 lung cancer cell lines established in either Japan or the USA. To validate the specificity and sensitivity of HPV detection methods, three cervical carcinoma cell lines were analyzed by the same methods. In 91 cell lines, the status of p53 mutations was comprehensively analyzed and the results were compared with several p53 databases to evaluate accurately the prevalence of p53 inactivation in lung cancers.

Materials and Methods

Patients and tissues. A total of 275 primary lung AdCs and 22 metastatic lung AdCs to the brain were obtained at surgery from patients treated at the National Cancer Center Hospital, Tokyo, and at Saitama Medical University Hospital. The tumors were pathologically diagnosed according to the tumor-node-metastasis classification of malignant tumors[15] (Table 1). Tumor tissues were stored at –80°C until DNA extraction, and genomic DNA was extracted as previously described.[16] This study was undertaken under the approval of the Institutional Review Board of the National Cancer Center.

Cell line DNA. DNA from 91 lung cancer cell lines[17,18] was screened for HPV-DNA in its genome. These cell lines consisted of 40 AdCs, 11 squamous cell carcinomas (SqCs), two adenosquamous carcinomas (ASCs), nine large-cell carcinomas (LCCs), 27 small-cell lung carcinomas (SCLCs), and two others (one carcinoid tumor and one neuroendocrine tumor), as listed in Table 2. Detailed information will be provided upon request. DNA from three cervical carcinoma cell lines, CaSki, SiHa, and HeLa, and HPV 33 containing plasmid DNA, was used as positive controls for detection of HPV-DNA.

Multiplex PCR with HPV type-specific primers. Sequences for the E1 and L2 regions of HPV 16 and for the E1 region of HPV 18 and 33, together with the aminolevulinate, delta-, synthase 1 (ALAS1) gene segment as an internal positive control, were simultaneously amplified by multiplex PCR in a single tube, as reported.[19] The primer sequences are shown in Supplementary Table S2. Multiplex PCR was performed with Takara Taq (Takara, Shiga, Japan) with a volume of 50 μL containing 1×

[3]To whom correspondence should be addressed.
E-mail: jyokota@ncc.go.jp

doi: 10.1111/j.1349-7006.2010.01622.x

Table 1. Clinicopathologic characteristics of lung adenocarcinomas

	PCR	Primary tumor		Brain metastasis
		Multiplex (%)	Nested (%)	Both (%)
No. of cases	–	275	138	22
Gender	Male	161 (59)	81 (59)	15 (68)
	Female	114 (41)	57 (41)	7 (32)
Age (years)	Mean	60.7	62.0	57.3
	Range	30–84	30–84	48–74
Pathological stage	I	201 (73)	124 (90)	–
	II	27 (10)	6 (4)	–
	III	45 (16)	8 (6)	–
	IV	2 (1)	0 (0)	–
Smoking history	Smoker	71 (55)	69 (58)	15 (68)
	Nonsmoker	57 (45)	51 (43)	7 (32)
	Unknown	147	18	0
p53 mutation	+	34 (32)	34 (33)	16 (73)
	–	72 (68)	70 (67)	6 (27)
	ND	169	34	0

ND, not determined.

PCR buffer, 2.5 mM $MgCl_2$, 0.2 mM dNTPs, 0.025 U Taq polymerase, 3 nM primers, and 10 ng template DNA. Amplifications were performed with the following cycling profiling using a GeneAmp PCR system 9700 apparatus (Applied Biosystems, Foster City, CA, USA): Taq polymerase activation by incubation at 95°C for 1 min, followed by 40 cycles of denaturation at 94°C for 30 s, annealing at 70°C for 90 s, and elongation at 72°C for 60 s. Five micro liters of the amplicons were analyzed by electrophoresis on 3% agarose gels and ethidium bromide staining.

Nested PCR with HPV type-specific primers. Sequences from the upstream regulatory region (URR) to the E7 region of HPV 16 and HPV 18 were first amplified by PCR with outer primers, and the HPV 16 E6/E7 and HPV 18 E6 regions were secondly amplified by nested PCR with inner primers, as reported previously.[20] The primer sequences are shown in Supplementary Table S2. The first round of PCR was performed under the following conditions: Taq polymerase activation at 95°C for 1 min, followed by 35 cycles of denaturation at 95°C for 1 min, annealing at 60°C for 1 min, and elongation at 72°C for 1 min. The second round of PCR was performed as follows: 95°C for 1 min, followed by 20 cycles of denaturation for 1 min at 95°C, 1 min of annealing at 60°C, and 1 min of elongation at 72°C. Polymerase chain reaction (PCR) was performed with a Takara Taq with a volume of 20 μL containing 1× PCR buffer, 0.2 mM dNTPs, 0.05 U Taq polymerase, 2 nM of primers, and 10 ng of template DNA for the first round PCR and 1 μL of the first round PCR products for the second round PCR using a GeneAmp PCR system 9700 apparatus (Applied Biosystems).

Mutation analysis of the *p53* gene. A total of 106 of the 275 primary lung AdCs and all of the 22 metastatic lung AdCs were previously examined for mutations in exons 4–8 of the *p53* gene by genomic PCR and direct sequencing.[21,22] All of the 91 lung cancer cell lines were examined for mutations in exons 2–11 covering all the coding sequences of the p53 gene by genomic PCR and direct sequencing as previously described.[18,23] Sequence data for the cell lines obtained in this study were compared with those of the Catalogue of Somatic Mutations in Cancer (COSMIC) (http://www.sanger.ac.uk/cosmic/).[24]

Results

Detection of HPV 16, 18, and 33 DNA by multiplex PCR. Recently, Nishiwaki *et al.* developed a rapid and sensitive multiplex PCR-based HPV genotyping method that allows the simultaneous amplification of 16 different HPV genotypes in a single tube reaction.[19] This method is based on the amplification of multiple HPV-DNA sequences with a set of HPV type-specific primers, and the HPV types are visually distinguished by the size of amplified fragments after separation by gel electrophoresis. Since DNA for HPV 16, 18, and 33 types has been frequently detected in lung AdC cells in East Asia, four primer sets for these three HPV types, in addition to a primer set for a control genome sequence, were used in this study. Two sets of primers were prepared for the amplification of the HPV 16 DNA[19] because of a possible high prevalence of HPV 16 DNA integration in lung AdC genomes.

The sensitivity and specificity of this method was validated using genomic DNA from three cervical cancer cell lines, CaSki, SiHa, and HeLa, and a lung cancer cell line, A549. Human papillomavirus (HPV) 16 has been shown to be integrated into chromosomal DNA in the CaSki and SiHa cell lines, while HPV 18 is integrated in the HeLa cell line.[25–27] A cell line with integration of HPV 33 was not available; therefore, HPV 33 containing plasmid DNA was mixed with A549 cell DNA as a ratio of one copy of HPV 33 DNA per diploid human genome. Specific DNA fragments for HPV 16, 18, and 33 of different sizes from each other were successfully amplified with the control genomic DNA fragment (Genome in Fig. 1) in CaSki, SiHa, and HeLa cells, as well as A549 cells mixed with HPV 33 DNA (Fig. 1). Two bands for HPV 16 DNA (HPV16-U and HPV16-L) were detected in CaSKi and SiHa cell DNA, while a band for HPV 18 DNA was detected in HeLa cell DNA. Human papillomavirus (HPV) 33-specific DNA was amplified from the mixture of plasmid DNA and A549 cell DNA, while no HPV-specific DNA was amplified from A549 cell DNA. Therefore, by this method, three different HPV types were successfully identified and distinguished by the difference in the sizes of amplified DNA. To determine the sensitivity of this method, each sample was serially diluted and mixed with A549 cell DNA to obtain genomic DNA with 0.1–1.0 copies of each HPV-DNA. Approximately 600 copies of HPV 16 DNA are integrated in CaSki cells, one to two copies of HPV 16 DNA are integrated in SiHa cells, and 20–50 copies of HPV 18 DNA are integrated in HeLa cells.[25–27] As shown in Figure 1, 0.1–1.0 copies of the HPV-DNA sequence per cell were detected by this method. Therefore, this method allowed us to detect one copy of HPV 16, 18, and/or 33 DNA integrated in chromosomal DNA of human cells. Further validation of this method was performed using DNA isolated from 18 primary cervical cancers because the presence of the HPV 16/18 DNA in these tumors was previously determined by Southern blot analysis.[28,29] Human papillomavirus (HPV) types detected by multiplex PCR analysis were completely the same as those by Southern blot analysis, and the sensitivity of multiplex PCR analysis for detection of HPV 16 DNA was higher than that of Southern blot analysis. Four cases negative for HPV 16 DNA by Southern blot analysis were positive by multiplex PCR analysis (data not shown). Therefore, we concluded that the sensitivity of the multiplex PCR analysis is higher than that of Southern blot analysis for detection of HPV 16 DNA in cancer cells.

We then applied this method for detection of HPV 16/18/33 DNA in 275 primary lung AdCs and 22 metastatic lung AdCs to the brain (Table 1). However, HPV-specific DNA was not amplified in any of these 297 lung AdCs. Thus, it was strongly suggested that HPV 16/18/33 DNA is not integrated in the chromosomal DNA of these lung AdCs.

Detection of HPV 16 and 18 DNA by nested PCR. It was reported that only a part of HPV-DNA, from the URR to the E6/E7 region, is commonly integrated in chromosomal DNA of cervical cancer cells, and that deletions of other regions occur in the course of viral DNA integration into host cell DNA.[25,26,30]

doi: 10.1111/j.1349-7006.2010.01622.x

Table 2. Status of the *p53* gene in 91 lung cancer cell lines

No.	Cell line	Hist.	Amino acid	Nucleotide
Point mutation				
1	ABC1	AdC	p.P278S	c.832C>T
2	CALU-3	AdC	p.M237I	c.711G>T
3	HCC44	AdC	p.S94X+ p.R175L	c.281C>G+ c.524G>T
4	HCC78	AdC	p.S241F	c.722C>T
5	HCC193	AdC	p.R248Q	c.743G>A
6	HCC515	AdC	p.L194F	c.580C>T
7	Ma10	AdC	p.G245V	c.734G>T
8	Ma17	AdC	p.Y126C	c.377A>G
9	Ma24	AdC	p.R337C	c.1009C>T
10	H23	AdC	p.M246I	c.738G>C
11	H441	AdC	p.R158L	c.473G>T
12	H820	AdC	p.T284P	c.850A>C
13	H1437	AdC	p.R267P	c.800G>C
14	H1975	AdC	p.R273H	c.818G>A
15	H2009	AdC	p.R273L	c.818G>T
16	H2087	AdC	p.V157F	c.469G>T
17	H2122	AdC	p.Q16L+ p.C176F	c.527G>T+ c.47A>T
18	H2126	AdC	p.E62X	c.184G>T
19	PC3	AdC	p.R282W	c.844C>T
20	PC7	AdC	p.H214R	c.641A>G
21	PC9	AdC	p.R248Q	c.743G>A
22	PC14	AdC	p.R248W	c.742C>T
23	RERF-LCMS	AdC	p.R248L	c.743G>T
24	RERF-LC-OK	AdC	p.F113C	c.338T>G
25	VMRC-LCD	AdC	p.R175H	c.524G>A
26	II-18	AdC	p.K164X	c.490A>T
27	H322	AdC	p.R248L	c.743G>T
28	EBC1	SqC	p.E171X	c.511G>T
29	LC1/Sq	SqC	p.M237I	c.711G>T
30	LK2	SqC	p.V272M	c.814G>A
31	HCC15	SqC	p.D259V	c.776A>T
32	H520	SqC	p.W146X	c.438G>A
33	SK-MES-1	SqC	p.E298X	c.892G>T
34	PC10	SqC	p.G245C	c.733G>T
35	HCC366	ASC	p.Y220C	c.659A>G
36	H596	ASC	p.G245C	c.733G>T
37	Lu65	LCC	p.E11Q	c.31G>C
38	Ma2	LCC	p.R175H	c.524G>A
39	Ma25	LCC	p.M237I	c.711G>T
40	H661	LCC	p.R158L+ p.S215I	c.473G>T+ c.644G>T
41	H1155	LCC	p.R273H	c.818G>A
42	PC13	LCC	p.G334V	c.1001G>T
43	HCC33	SCLC	p.C242Y	c.725G>A
44	Lu134	SCLC	p.P278L	c.833C>T
45	Lu135	SCLC	p.G244C	c.730G>T
46	Lu139	SCLC	p.V157F	c.469G>T
47	N417	SCLC	p.E298X	c.892G>T
48	H69	SCLC	p.E171X	c.511G>T
49	H128	SCLC	p.E62X	c.184G>T
50	H345	SCLC	p.Y236C	c.707A>G
51	H446	SCLC	p.Q154V	c.461G>T
52	H841	SCLC	p.C242S	c.724A>T
53	H1184	SCLC	p.G334V	c.1001G>T
54	H1450	SCLC	p.L194R	c.581T>G
55	H1607	SCLC	p.P151H	c.452C>A
56	H1963	SCLC	p.V147D+ p.H214R	c.440T>A+ c.641A>G
57	H2107	SCLC	p.K101X	c.301A>T
58	H2141	SCLC	p.R209X	c.625A>T
59	H2171	SCLC	p.Q144X	c.430C>T
60	H2195	SCLC	p.V157F	c.469G>T
61	H1618	SCLC	p.R248L	c.743G>T
62	H187	SCLC	p.S241C	c.722C>G
63	H510	SCLC	p.R282G	c. 844C>G
64	H1770	Neuroendocrine	p.R248W	c.741-742CC>TT
Small insertion/deletion (≤9 nucleotides)				
1	Ma29	AdC	p.V121fs	c.363delT
2	H522	AdC	p.P191fs	c.572delC
3	H1648	AdC	p.L35fs	c.103-104insT
4	HCC95	SqC	p.G334fs	c.1000(-1003) 1G del
5	H157	SqC	p.L35fs+ p.E298X	c.103-104insT+ c.892G>T
6	H727	Carcinoid	p.Q165-S166 insYKQ	c.496-497ins9
Large deletion				
1	H358	AdC	p?	Large deletion
2	H1299	LCC	p?	Large deletion
Splicing-site mutation				
1	H1703	AdC	p.G262fs	g. Ivs8 +1g>t
2	H1819	AdC	p.A307fs	g. Ivs9 +1g>t
3	H2347	AdC	p.Y126fs	g.375G>A
4	H1650	AdC	p.V225fs	g.Ivs6 -2a>g
5	Sq1	SqC	p.Y126fs	g. Ivs4 +2t>c
6	H82	SCLC	p.Y126fs	g.375G>T
7	H209	SCLC	p.V225fs	g. Ivs6 -2a>t
8	H526	SCLC	p.S33fs	g. Ivs3 -1g>c
9	H1339	SCLC	p.I332fs	g.Ivs9 +1g>t
Wild type				
1	A427	AdC	—	—
2	A549	AdC	—	—
3	Ma12	AdC	—	—
4	Ma26	AdC	—	—
5	H1395	AdC	—	—
6	H226	SqC	—	—
7	Lu99A	LCC	—	—
8	H460	LCC	—	—
9	Lu24	SCLC	—	—
10	Ms18	SCLC	—	—

p, c, and g indicate protein, cDNA, and genomic DNA.
AdC, adenocarcinoma; ASC, adenosquamous carcinoma; LCC, large-cell carcinoma;
SCLC, small-cell lung carcinoma; SqC, squamous cell carcinoma.

The primers for HPV 16, 18, and 33 in the above multiplex PCR analysis were designed to amplify the E1 or L2 region (Supplementary Table S2).[19] Therefore, it was possible that multiplex PCR analysis failed to detect the HPV-DNA sequences because of integration of truncated HPV genomes without the E1 and L2 regions into host cell DNA. To pursue the possible integration of HPV 16 and 18 DNA in lung AdC cells, we performed a nested PCR analysis for the E6 and E7 regions of HPV 16 and 18. The URR to the E7 region of both HPV 16 and 18 genomes was first amplified using outer primers, then, the E6 to E7 region of the HPV 16 DNA and the E6 region of the HPV 18 DNA were amplified using inner primers (Supplementary Table S2), respectively, according to the method previously described.[20] As in the multiplex PCR analysis, HPV 16- and 18-specific DNA fragments were successfully amplified from the CaSki, SiHa, and HeLa cell lines, but not from A549. Next, 138 of the 275 primary AdCs and all of the 22 metastatic AdCs used for

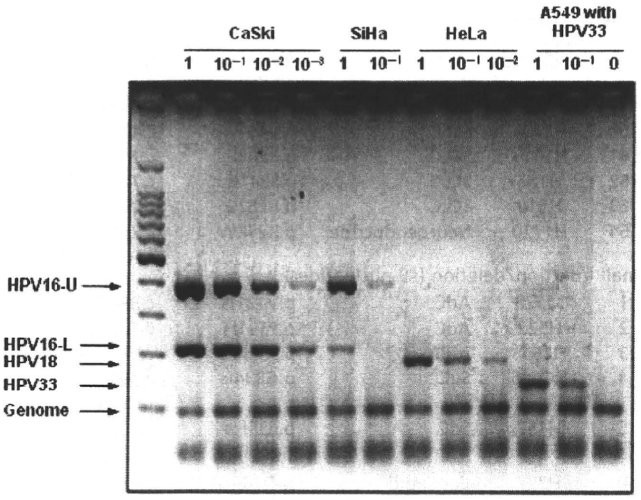

Fig. 1. Detection of human papillomavirus (HPV) 16, 18, and 33 DNA in cervical cancer cell lines by multiplex PCR analysis. Specificity and sensitivity for detection of HPV 16, 18, and 33 DNA. Polymerase chain reaction (PCR) was performed using DNA from CaSki (~600 copies of HPV 16 integrated), SiHa (1–2 copies of HPV 16 integrated), HeLa (20–50 copies of HPV 18 integrated), and A549 cells with/without HPV 33 containing plasmid DNA. Each sample was serially diluted with A549 cell DNA up to the copy number of 0.1–1.0 per cell for HPV-DNA. Five micro liters of the amplicons were analyzed by electrophoresis on 3% agarose gels and ethidium bromide staining. 100 bp DNA Ladder (Takara, Shiga, Japan) was used as a size marker.

multiplex PCR analysis were subjected to nested PCR analysis (Table 1). However, none of them showed positive signals for the E6/E7 regions of the HPV 16 or 18. The results of multiplex PCR analysis as well as those of nested PCR analysis strongly indicated that HPV 16 and 18 are not integrated in lung AdCs developed in Japan, at least in the Tokyo area.

Absence of HPV 16, 18, and 33 DNA sequences in lung cancer cell lines. We next attempted to detect HPV 16, 18, and 33 DNA in a panel of 91 human lung cancer cell lines established in either Japan or the USA. Among the 91 cell lines, 30 originated from Japanese, 42 from Caucasians, and five from African-Americans. Detailed information was not available for the remaining 14 cell lines. Forty cell lines were derived from AdC and the remaining 51 were from other histological types. Both multiplex PCR and nested PCR were performed on all of these cell lines. However, no HPV-specific signals were obtained in any of these cell lines. Therefore, HPV 16, 18, and 33 DNA is not integrated in the 91 lung cancer cell lines established in Japan and the USA. Eleven cell lines were derived from SqC, and 27 cell lines were derived from SCLC; therefore, HPV 16/18/33 integration was not evident in any major histological types of lung cancer.

Status of p53 mutations in lung cancer cell lines. We previously examined for p53 mutations in 106 of the 275 primary tumors and all 22 brain metastases,[21,22] and the mutations were detected in 34 of the 106 primary tumors (32%) and 16 of the 22 brain metastases (73%) (Table 1). We recently reported the status of p53 mutations in 87 of the 91 cell lines analyzed in the present study.[18] In that study, mutation data of several cell lines were obtained not only by direct sequencing of the p53 coding regions but also from the COSMIC database, and the mutations were detected in 70 of the 87 cell lines (80%). However, during this study, we noticed that data for p53 mutations are not the same among three major databases, COSMIC, UMD_TP53 database (http://p53.free.fr), and IARC p53 database (http://www-p53.iarc.fr).[24,31,32] Absence of HPV 16/18/33 integration as well as p53 mutations in 17 lung cancer cell lines prompted us to re-investigate the status of p53 mutations in these cell lines. Therefore, the p53 mutation status in all the 91 cell lines was determined by direct sequencing of all the coding exons, from exon 2 to exon 11, together with exon–intron boundaries of these exons (Table 2). If mutations were detected in the exon–intron boundaries, a possible occurrence of splicing abnormalities due to the mutations was examined by direct sequencing of p53 cDNA products from the corresponding cell lines. Point mutations were detected in 64 of the 91 cell lines, small insertions/deletions in six of them, and large deletions in two of them. Splice-site mutations were detected in nine cell lines, in which shifts of open reading frames due to either exon skipping or intron retention were confirmed. Accordingly, only 10 cell lines were shown to carry the wild-type *p53* gene and express normal p53 protein, including five of the 40 AdC cell lines.

The status of 36 cell lines was not available in COSMIC and thus was defined by our studies (Supplementary Table S3-1) ([18,21–23], this study). The status of 45 cell lines was concordant between our data and COSMIC data (Supplementary Table S3-2), whereas that of the remaining 10 cell lines was discordant (Supplementary Table S3-3). Therefore, although 10 of the 91 lung cancer cell lines carry the wild-type *p53* gene, HPV 16, 18, or 33 are not integrated in these cell lines.

Discussion

To detect HPV-DNA in lung cancer cells, we applied two different PCR methods with HPV type-specific primers, one-step multiplex PCR[19] and nested PCR,[20] because PCR with type-specific primers was reported to be more sensitive than PCR with consensus primers to detect HPV-DNA sequences in human cell DNA.[7] The prevalence and genotype distribution of HPV in cervical cancer precursor lesions defined by one-step multiplex PCR was reported to be compatible with several previous data.[19] In addition, by using these methods, HPV 16 and 18 DNA was distinguishably and efficiently amplified from three cervical cancer cell lines. Therefore, the lack of HPV 16, 18, and 33 DNA in primary lung AdC as well as in lung cancer cell lines would not be due to the low sensitivity of this method for HPV detection. Accordingly, it was concluded from this study that HPV 16, 18, and 33 are not (or are rarely) integrated in lung AdC genomes in the Japanese, particularly those living in the Tokyo area. Lung cancer cell lines analyzed in this study have been established in either Japan or the USA, and consist of all major histological types of lung cancer. Absence of HPV 16/18/33 infection in primary lung AdCs in the US population and lung cancer cell lines established in the USA was previously reported.[33–35] Therefore, the results in the cell lines are consistent with the results in primary AdCs in both Japan and the USA. Indeed, we further attempted to detect HPV-associated DNA sequences in these cell lines by PCR under several low stringent conditions using a set of consensus primers for HPV 16, 18, and 33. However, no HPV-specific signals were detected in any of the 91 lung cancer cell lines examined (data not shown). Therefore, we concluded that no HPV 16/18/33 DNA is integrated in these cell lines. Accordingly, HPV infection seems not to play an important role in the development of lung cancer in Japan nor in the USA, although it is still possible that other HPV types play some role in its development.

A Taiwanese study reported that female never-smokers with lung cancer who were older than 60 years of age had a significantly higher prevalence of HPV 16/18 infections.[8] However, in Korean lung cancer patients, HPV 16/18/33 infections were not associated with gender, smoking status, and histological type.[10] In a study in China, HPV 16/18 infections were not correlated with any clinicopathological parameter, including

doi: 10.1111/j.1349-7006.2010.01622.x

age, gender, smoking status, and histological type, either.[9] In this study, 41% (121/297) and 43% (64/150) of AdC patients were female and non-smokers, respectively (Table 1). Therefore, the etiological role of HPV 16/18 in lung carcinogenesis in non-smokers seems to be restricted to certain geographic areas, and in Japan, HPV 16/18 infection does not play a causative role in the development of lung AdC in female non-smokers.

An inverse correlation of HPV 16/18 E6 protein expression with p53 expression was also reported in Taiwanese lung tumors.[36] However, in a study in China, there was a relationship between the presence of HPV 16/18 DNA and abnormal p53 protein accumulation.[37] Therefore, association of HPV infection with p53 inactivation is still unclear in lung cancer. We previously examined for p53 mutations in 128 of 297 lung AdCs analyzed in this study, and the mutations were detected in 50 cases (39%) (Table 1); therefore, it was possible that HPV is infected in another 78 cases. However, none of the 78 lung AdCs carried HPV 16/18/33 DNA in their genomes. Accordingly, HPV 16/18/33 infections appear to play a limited role in the development of lung AdC in Japan. These results prompted us to analyze comprehensively the status of the *p53* gene in a large panel of lung cancer cell lines. The *p53* gene is inactivated not only by mutations in the coding regions, but also by splicing abnormalities caused by mutations in the exon–intron boundaries and homozygous deletions, and the incidence of p53 genetic alterations in total was 89% (81/91). Therefore, although 10 of the 91 cell lines were shown to carry the wild-type *p53* gene, no HPV 16/18/33 DNA was detected in these cell lines. Since the status of the *p53* gene in these cell lines was not consistent among several databases and reports, the results provided here will be highly informative to diverse scientists using these cell lines for molecular and biological studies.

In Japan, HPV-DNA has been detected in <10% of lung AdC in Chiba and Hokkaido, and ~20% in Okinawa (Supplementary Table S1). Therefore, we cannot totally rule out the involvement of HPV infection in the etiology of lung AdC in Japan. However, the present results strongly indicate that HPV infection plays only a limited role, if any, in the development of lung AdC in Japan.

Acknowledgments

This work was supported by Grants-in-Aid from the Ministry of Health, Labor and Welfare for the 3rd-Term Comprehensive 10-year Strategy for Cancer Control and for Cancer Research (16-1) and a Grant-in-Aid for the Program for Promotion of Fundamental Studies in Health Sciences of the National Institute of Biomedical Innovation (NiBio). We are grateful to Drs R. Nishikawa and K. Mishima of the Saitama Medical University Hospital for preparation of metastatic lung adenocarcinoma specimens.

Disclosure Statement

The authors have no conflict of interest.

References

1 zur Hausen H. Papillomaviruses in the causation of human cancers - a brief historical account. *Virology* 2009; **384**: 260–5.
2 Werness BA, Levine AJ, Howley PM. Association of human papillomavirus types 16 and 18 E6 proteins with p53. *Science* 1990; **248**: 76–9.
3 Scheffner M, Werness BA, Huibregtse JM, Levine AJ, Howley PM. The E6 oncoprotein encoded by human papillomavirus types 16 and 18 promotes the degradation of p53. *Cell* 1990; **63**: 1129–36.
4 Nakanishi H, Matsumoto S, Iwakawa R *et al.* Whole genome comparison of allelic imbalance between noninvasive and invasive small-sized lung adenocarcinomas. *Cancer Res* 2009; **69**: 1615–23.
5 Sun S, Schiller JH, Gazdar AF. Lung cancer in never smokers–a different disease. *Nat Rev Cancer* 2007; **7**: 778–90.
6 Klein F, Kotb WF, Petersen I. Incidence of human papilloma virus in lung cancer. *Lung Cancer* 2009; **65**: 13–8.
7 Srinivasan M, Taioli E, Ragin CC. Human papillomavirus type 16 and 18 in primary lung cancers–a meta-analysis. *Carcinogenesis* 2009; **30**: 1722–8.
8 Cheng YW, Chiou HL, Sheu GT *et al.* The association of human papillomavirus 16/18 infection with lung cancer among nonsmoking Taiwanese women. *Cancer Res* 2001; **61**: 2799–803.
9 Fei Y, Yang J, Hsieh WC *et al.* Different human papillomavirus 16/18 infection in Chinese non-small cell lung cancer patients living in Wuhan, China. *Jpn J Clin Oncol* 2006; **36**: 274–9.
10 Park MS, Chang YS, Shin JH *et al.* The prevalence of human papillomavirus infection in Korean non-small cell lung cancer patients. *Yonsei Med J* 2007; **48**: 69–77.
11 Hirayasu T, Iwamasa T, Kamada Y, Koyanagi Y, Usuda H, Genka K. Human papillomavirus DNA in squamous cell carcinoma of the lung. *J Clin Pathol* 1996; **49**: 810–7.
12 Miyagi J, Kinjo T, Tsuhako K *et al.* Extremely high Langerhans cell infiltration contributes to the favourable prognosis of HPV-infected squamous cell carcinoma and adenocarcinoma of the lung. *Histopathology* 2001; **38**: 355–67.
13 Kinoshita I, Dosaka-Akita H, Shindoh M *et al.* Human papillomavirus type 18 DNA and E6-E7 mRNA are detected in squamous cell carcinoma and adenocarcinoma of the lung. *Br J Cancer* 1995; **71**: 344–9.
14 Hiroshima K, Toyozaki T, Iyoda A *et al.* Ultrastructural study of intranuclear inclusion bodies of pulmonary adenocarcinoma. *Ultrastruct Pathol* 1999; **23**: 383–9.
15 Sobin LH, Wittekind CH, eds. *TNM classification of malignant tumours*, 6th ed. New York: Wiley-Liss; 2002: p. 99–103.
16 Sakamoto H, Mori M, Taira M *et al.* Transforming gene from human stomach cancers and a noncancerous portion of stomach mucosa. *Proc Natl Acad Sci U S A* 1986; **83**: 3997–4001.
17 Kohno T, Otsuka A, Girard L *et al.* A catalog of genes homozygously deleted in human lung cancer and the candidacy of PTPRD as a tumor suppressor gene. *Genes Chromosomes Cancer* 2010; **49**: 342–52.
18 Blanco R, Iwakawa R, Tang M *et al.* A gene-alteration profile of human lung cancer cell lines. *Hum Mutat* 2009; **30**: 1199–206.
19 Nishiwaki M, Yamamoto T, Tone S *et al.* Genotyping of Human Papillomaviruses by a Novel One-Step Typing Method with Multiplex PCR and Clinical Applications. *J Clin Microbiol* 2008; **46**: 1161–8.
20 Wu EQ, Zhang GN, Yu XH *et al.* Evaluation of high-risk human papillomaviruses type distribution in cervical cancer in Sichuan province of China. *BMC Cancer* 2008; **8**: 202.
21 Tomizawa Y, Kohno T, Fujita T *et al.* Correlation between the status of the p53 gene and survival in patients with stage I non-small cell lung carcinoma. *Oncogene* 1999; **18**: 1007–14.
22 Iwakawa R, Kohno T, Anami Y *et al.* Association of p16 homozygous deletions with clinicopathological characteristics and EGFR/KRAS/p53 mutations in lung adenocarcinoma. *Clin Cancer Res* 2008; **14**: 3746–53.
23 Matsumoto S, Iwakawa R, Takahashi K *et al.* Prevalence and specificity of LKB1 genetic alterations in lung cancers. *Oncogene* 2007; **26**: 5911–8.
24 Forbes SA, Tang G, Bindal N *et al.* COSMIC (the Catalogue of Somatic Mutations in Cancer): a resource to investigate acquired mutations in human cancer. *Nucleic Acids Res* 2010; **38**(Database issue): D652–7.
25 Schwarz E, Freese UK, Gissmann L *et al.* Structure and transcription of human papillomavirus sequences in cervical carcinoma cells. *Nature* 1985; **314**: 111–4.
26 Baker CC, Phelps WC, Lindgren V, Braun MJ, Gonda MA, Howley PM. Structural and transcriptional analysis of human papillomavirus type 16 sequences in cervical carcinoma cell lines. *J Virol* 1987; **61**: 962–71.
27 Yee C, Krishnan-Hewlett I, Baker CC, Schlegel R, Howley PM. Presence and expression of human papillomavirus sequences in human cervical carcinoma cell lines. *Am J Pathol* 1985; **119**: 361–6.
28 Yokota J, Tsukada Y, Nakajima T *et al.* Loss of heterozygosity on the short arm of chromosome 3 in carcinoma of the uterine cervix. *Cancer Res* 1989; **49**: 3598–601.
29 Kohno T, Takayama H, Hamaguchi M *et al.* Deletion mapping of chromosome 3p in human uterine cervical cancer. *Oncogene* 1993; **8**: 1825–32.
30 Pett M, Coleman N. Integration of high-risk human papillomavirus: a key event in cervical carcinogenesis? *J Pathol* 2007; **212**: 356–67.
31 Berglind H, Pawitan Y, Kato S, Ishioka C, Soussi T. Analysis of p53 mutation status in human cancer cell lines: a paradigm for cell line cross-contamination. *Cancer Biol Ther* 2008; **7**: 699–708.
32 Petitjean A, Mathe E, Kato S *et al.* Impact of mutant p53 functional properties on TP53 mutation patterns and tumor phenotype: lessons from recent developments in the IARC TP53 database. *Hum Mutat* 2007; **28**: 622–9.

33 Yousem SA, Ohori NP, Sonmez-Alpan E. Occurrence of human papillomavirus DNA in primary lung neoplasms. *Cancer* 1992; **69**: 693–7.
34 Wistuba II, Behrens C, Milchgrub S *et al.* Comparison of molecular changes in lung cancers in HIV-positive and HIV-indeterminate subjects. *JAMA* 1998; **279**: 1554–9.
35 Shimizu E, Coxon A, Otterson GA *et al.* RB protein status and clinical correlation from 171 cell lines representing lung cancer, extrapulmonary small cell carcinoma, and mesothelioma. *Oncogene* 1994; **9**: 2441–8.
36 Cheng YW, Wu MF, Wang J *et al.* Human papillomavirus 16/18 E6 oncoprotein is expressed in lung cancer and related with p53 inactivation. *Cancer Res* 2007; **67**: 10686–93.
37 Wang Y, Wang A, Jiang R *et al.* Human papillomavirus type 16 and 18 infection is associated with lung cancer patients from the central part of China. *Oncol Rep* 2008; **2**: 333–9.

Supporting Information

Additional Supporting Information may be found in the online version of this article:

Table S1. Prevalence of human papillomavirus (HPV) 16, 18, and 33 in lung adenocarcinomas in East Asia.

Table S2. Primer sequences for detection of human papillomavirus (HPV) DNA in cancer cell DNA.

Table S3-1. p53 status defined in our studies but not registered in the COSMIC database.

Table S3-2. Concordance of p53 status defined in our studies and registered in the COSMIC database.

Table S3-3. Discordance of p53 status defined in our studies and registered in the COSMIC database.

Please note: Wiley-Blackwell are not responsible for the content or functionality of any supporting materials supplied by the authors. Any queries (other than missing material) should be directed to the corresponding author for the article.

doi: 10.1111/j.1349-7006.2010.01622.x

The EMBO Journal (2010) 29, 2802–2812 | © 2010 European Molecular Biology Organization | All Rights Reserved 0261-4189/10
www.embojournal.org

THE EMBO JOURNAL

14-3-3γ mediates Cdc25A proteolysis to block premature mitotic entry after DNA damage

Kousuke Kasahara[1], Hidemasa Goto[1,2], Masato Enomoto[1,2], Yasuko Tomono[3], Tohru Kiyono[4] and Masaki Inagaki[1,2,*]

[1]Division of Biochemistry, Aichi Cancer Center Research Institute, Nagoya, Aichi, Japan, [2]Department of Cellular Oncology, Nagoya University Graduate School of Medicine, Nagoya, Aichi, Japan, [3]Division of Molecular and Cell Biology, Shigei Medical Research Institute, Okayama, Okayama, Japan and [4]Virology Division, National Cancer Center Research Institute, Chuo-ku, Tokyo, Japan

14-3-3 proteins control various cellular processes, including cell cycle progression and DNA damage checkpoint. At the DNA damage checkpoint, some subtypes of 14-3-3 (β and ζ isoforms in mammalian cells and Rad24 in fission yeast) bind to Ser345-phosphorylated Chk1 and promote its nuclear retention. Here, we report that 14-3-3γ forms a complex with Chk1 phosphorylated at Ser296, but not at ATR sites (Ser317 and Ser345). Ser296 phosphorylation is catalysed by Chk1 itself after Chk1 phosphorylation by ATR, and then ATR sites are rapidly dephosphorylated on Ser296-phosphorylated Chk1. Although Ser345 phosphorylation is observed at nuclear DNA damage foci, it occurs more diffusely in the nucleus. The replacement of endogenous Chk1 with Chk1 mutated at Ser296 to Ala induces premature mitotic entry after ultraviolet irradiation, suggesting the importance of Ser296 phosphorylation in the DNA damage response. Although Ser296 phosphorylation induces the only marginal change in Chk1 catalytic activity, 14-3-3γ mediates the interaction between Chk1 and Cdc25A. This ternary complex formation has an essential function in Cdc25A phosphorylation and degradation to block premature mitotic entry after DNA damage.

The EMBO Journal (2010) **29**, 2802–2812. doi:10.1038/emboj.2010.157; Published online 16 July 2010
Subject Categories: cell cycle; genome stability & dynamics
Keywords: Cdc25; Chk1; DNA damage checkpoint; phosphorylation; 14-3-3

Introduction

The cell cycle checkpoint is a fundamental mechanism, not only for monitoring genomic stability, but also for coordinating repair and cell cycle progression. The protein kinase cascade from ATR to Chk1 has important functions in the DNA damage checkpoint (Zhou and Elledge, 2000; Bartek and Lukas, 2003; Kastan and Bartek, 2004). In response to damaged DNA or stalled replication, ATR phosphorylates Chk1 at Ser317 and Ser345; this phosphorylation is considered to elevate the catalytic activity of Chk1 (Zhao and Piwnica-Worms, 2001; Walker *et al*, 2009). Chk1 then phosphorylates and inhibits Cdc25 family phosphatases, which consist of Cdc25A, B and C in human cells (Boutros *et al*, 2007). For example, Chk1 induces Cdc25A-Ser76 phosphorylation, which results in βTrCP-dependent Cdc25A degradation (Busino *et al*, 2003, 2004; Jin *et al*, 2003; Neely and Piwnica-Worms, 2003; Melixetian *et al*, 2009). As Cdc25 dephosphorylates cyclin-dependent kinases (Cdks) at an inhibitory phosphorylation site (Cdk1 at Tyr15), Cdc25 inhibition results in Cdk inactivation and cell cycle arrest (Jackman and Pines, 1997; Zhou and Elledge, 2000; Bartek and Lukas, 2003; Kastan and Bartek, 2004).

The DNA damage checkpoint response is also modulated by phosphoserine/phosphothreonine-binding proteins/domains, such as 14-3-3 proteins, FHA domains and BRCT domains (Mohammad and Yaffe, 2009). Studies in fission yeast first suggested that there was a correlation between 14-3-3 proteins and checkpoint control: Rad24, one of 14-3-3 proteins in fission yeast, was identified in a search for irradiation-sensitive mutants (Ford *et al*, 1994). Further studies indicated that Chk1 and 14-3-3 proteins act through Cdc25 (Pines, 1999). In both human cells and fission yeast, Chk1 phosphorylates Cdc25 on a conserved serine residue (human Cdc25C on Ser216), creating a phosphoserine-binding site for 14-3-3 (Furnari *et al*, 1997; Peng *et al*, 1997; Sanchez *et al*, 1997). As Ser216 on human Cdc25C appears to be highly phosphorylated by C-TAK1 in the absence of DNA damage (Peng *et al*, 1998; Russell, 1998; Zhou and Elledge, 2000), it remains controversial how 14-3-3 modulates the signal from Chk1 to Cdc25 in mammals.

Some subtypes of 14-3-3 (β and ζ isoforms in mammalian cells and Rad24 in fission yeast) also bind Chk1 in a Ser345-phosphorylation-dependent manner (Jiang *et al*, 2003; Dunaway *et al*, 2005). This binding promotes the nuclear retention of Chk1 likely through the masking of NES on Chk1 (Jiang *et al*, 2003; Dunaway *et al*, 2005). As Chk1 is phosphorylated at several sites other than Ser317 and Ser345 (ATR sites) in DNA damage responses (Clarke and Clarke, 2005; Puc *et al*, 2005; Ikegami *et al*, 2008), we postulate that Chk1 phosphorylation at other site(s) may also modulate the checkpoint signalling through 14-3-3 binding. Here, we show that the γ subtype of 14-3-3 also forms a complex with Chk1 when DNA damage occurs. This binding depends on Chk1 autophosphorylation at Ser296, which occurs after ATR-induced phosphorylation of Chk1 (by implication, catalytic activation of Chk1) and then promotes dephosphorylation at the ATR sites. This phosphorylation shift from ATR sites to Ser296 not only has an important function in the spread of Chk1 signals, but also changes the Chk1-binding subtype of 14-3-3 (from β or ζ to γ). The 14-3-3γ serves as a platform between Cdc25A and Ser296-phosphorylated Chk1, promoting Chk1-induced Cdc25A phosphorylation at Ser76, a critical site for its degradation.

*Corresponding author. Division of Biochemistry, Aichi Cancer Center Research Institute, 1-1 Kanokoden, Chikusa-ku, Nagoya, Aichi 464-8681, Japan. Tel: +81 52 762 6111/ext. 7020; Fax: +81 52 763 5233; E-mail: minagaki@aichi-cc.jp

Received: 14 January 2010; accepted: 21 June 2010; published online: 16 July 2010

Results

Ser296 phosphorylation is catalysed by Chk1 itself after phosphorylation by ATR

Chk1 was reported to be phosphorylated not only at Ser317 and Ser345, but also at Ser296 (Clarke and Clarke, 2005) in response to DNA damage, but only limited information has been available about Ser296 phosphorylation. We first produced an antibody that specifically recognizes Chk1 phosphorylated at Ser296 (Figure 1A and B; see also Supplementary Figure S1). Using Chk1 purified from baculovirus-infected Sf9 cells, we performed the *in vitro* autophosphorylation assay. After 30 min of the incubation with [γ-^{32}P] ATP, radioactive phosphates (^{32}P) were incorporated

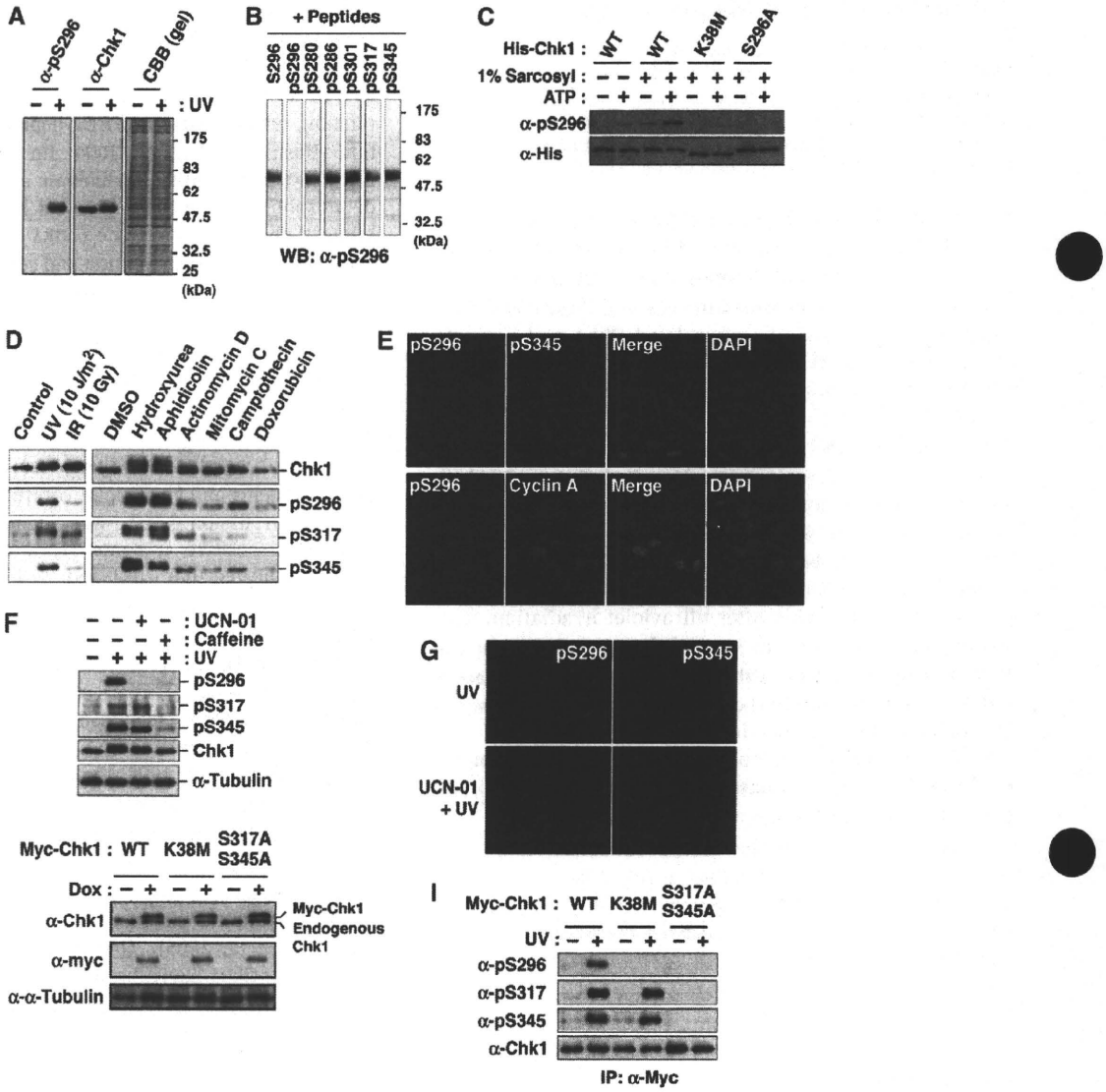

Figure 1 Chk1 autophosphorylation at Ser296. (**A**, **B**) Characterization of an antibody specifically recognizing Chk1 phosphorylation at Ser296. The antibody (α-pS296) reacted specifically with a band corresponding to Chk1 in lysates of UV-irradiated (+) HeLa cells (Ikegami *et al*, 2008), but not of non-treated (−) cells (**A**). Immunoreactivity was impaired specifically by preincubation with pS296 corresponding to Ser296-phosphorylated Chk1, but not with non-phosphorylated peptide S296 and phosphopeptides for other sites within Chk1 (**B**). (**C**) The *in vitro* autophosphorylation assay using 6xHis-ProS2-Chk1 (His-Chk1) expressed in bacteria. *E. coli* strain BL21-CodonPlus®(DE3)-RP was transformed with pCold ProS2 carrying each Chk1. Each 6xHis-ProS2-tagged Chk1 was expressed in the presence of 1 mM IPTG at 15°C for 16 h. *E. coli* cells were lysed in the lysis buffer (40 mM Hepes-NaOH [pH 8.0], 300 mM NaCl, 1% Triton X-100) supplemented with (+) or without (−) 1% sarcosyl. After centrifugation (17 000 *g*) for 10 min at 4°C, the supernatant was rotated with TALON metal affinity resin at 4°C for 1 h. After washing with the lysis buffer and reaction buffer (25 mM Tris–HCl [pH 7.5], 10 mM $MgCl_2$), the beads were incubated in the reaction buffer with (+) or without (−) 10 μM ATP at 30°C for 30 min. Chk1 phosphorylated at Ser296 or total Chk1 was detected through immunoblotting with an anti-pS296 (α-pS296) or anti-His (α-His) antibody, respectively. (**D**) HeLa cells were irradiated with UV, X-rays (IR; 10 Gy) or none (control) and then incubated for an additional 1 h. For treatment with drugs, cells were incubated with 2 mM hydroxyurea, 5 μg/ml aphidicolin, 5 μM actinomycin D, 5 μM mitomycin C, 5 μM camptothecin, 10 μM doxorubicin or 0.1% DMSO (as a solvent control) for 3 h. Extracts were subjected to immunoblotting with the indicated antibodies. (**E**) HeLa cells irradiated with UV were stained with the indicated antibodies and DAPI. (**F**, **G**) Immunoblots (**F**) or immunocytochemistry (**G**) shows effects of pre-treatment with UCN-01 or caffeine on Chk1 phosphorylation in UV-irradiated HeLa cells. (**H**, **I**) Establishment of HeLa cells in which each Myc-Chk1 (WT, K38 M or S317A/S345A) is expressed in a doxycycline (Dox)-dependent manner (**H**). Levels of Chk1 phosphorylation after UV-irradiation (**I**).

into Chk1 wild-type (WT) protein (Supplementary Figure S1E). The electrophoretic mobility of Chk1 was slower after the incubation with ATP; the anti-pS296 on Chk1 (α-pS296) reacted with WT specifically after the incubation (Supplementary Figure S1E). Chk1 mutation at Lys38 to Met (K38M), which lost the catalytic activity, almost completely abolished ^{32}P incorporation, the mobility shift and α-pS296 immunoreactivity (Supplementary Figure S1E). Chk1 mutation at Ser296 to Ala (S296A) reduced ^{32}P incorporation and abolished α-pS296 immunoreactivity. However, S296A did not completely abolish both ^{32}P incorporation and the mobility shift (Supplementary Figure S1E). In the 2D phosphopeptide mapping analysis, S296A induced the disappearance of the radioactive spots 1 and 2, although other major spots (3–6) appeared to remain unchanged on the thin layer plate (Supplementary Figure S1E). To rule out the possibility that a contaminating kinase in insect cells may phosphorylate Chk1-Ser296, we used His-ProS2-Chk1 protein expressed in bacteria (Figure 1C; His-Chk1). In the extraction of protein without sarcosyl, α-pS296 immunoreactivity in WT was observed very weakly even after the incubation with ATP (Figure 1C; 1% sarcosyl: −). On the other hand, the extraction of WT protein with 1% sarcosyl elevated the α-pS296 immunoreactivity after the incubation with ATP much more than without ATP (Figure 1C) (Zhao and Piwnica-Worms, 2001). However, such phenomena were not observed in the case of K38M or S296A (Figure 1C). All these results suggested that Ser296 on Chk1 serves as one of the major autophosphorylation sites *in vitro*.

We next examined Ser296 phosphorylation in the checkpoint response. In response to various DNA damage stimuli and replication disorders, Chk1 phosphorylation at Ser296 was found to occur in a way similar to the phosphorylation at ATR sites (Figure 1D and E). Furthermore, treatment with UCN-01 (a Chk1 kinase inhibitor) attenuated Chk1 phosphorylation at Ser296, but not at ATR sites, although caffeine (an ATR and ATM inhibitor) showed non-specific reduction in phosphorylation rates (Figure 1F and G). Next, we established HeLa cell lines in which Myc-tagged Chk1 was expressed in a tetracycline- or doxycycline (Dox)-dependent manner; the protein level of each exogenous Chk1 was very similar to that of endogenous Chk1 under our experimental conditions (Figure 1H). Although Ser296 phosphorylation in response to ultraviolet (UV) irradiation was observed in WT, it rarely occurred on Chk1 mutated at ATR sites to Ala (S317A/S345A; Figure 1I). In a kinase dead Chk1 mutant (K38M), Ser296 phosphorylation was hardly detected, although Ser317 and Ser345 phosphorylation was observed (Figure 1I). The above observations suggested that Chk1 phosphorylation at Ser296 is catalysed by its own kinase activity, but not by ATR, although it requires pre-phosphorylation at ATR sites, which has implications for the catalytic activation of Chk1 (Zhao and Piwnica-Worms, 2001; Walker *et al*, 2009).

Ser296-phosphorylated Chk1 is rapidly dephosphorylated at ATR sites and distributed throughout the nucleoplasm

We then scrutinized the subcellular distribution of Ser296-phosphorylated Chk1. In UV-irradiated cells, Ser345-phosphorylated Chk1 was observed at nuclear foci of ATR-interacting protein (ATRIP) and the phosphorylated form of RPA32 (an ATR substrate; Figure 2A), in which ATR is considered to be activated (Zou and Elledge, 2003). In contrast, Ser296-phosphorylated Chk1 appeared to distribute diffusely in the nucleus (Figure 2B). In support of this observation, nuclear signals of anti-pS296, but not of anti-pS345, almost completely disappeared after brief extraction with Triton X-100 detergent (Figure 2C). Biochemical fractionation (Figure 2D) also showed that Ser296-phosphorylated Chk1 was clearly detectable in the soluble (S1 plus S2) but not the chromatin (P2) fractions, although Ser317- and Ser345-phosphorylated Chk1 existed in both (Jiang *et al*, 2003; Smits *et al*, 2006). These observations suggest that Ser296-phosphorylated Chk1 is distributed throughout the nucleoplasm, distinct from the localization of Chk1 phosphorylated by ATR.

We further confirmed that only faint signals for anti-pS317/pS345 and -pS296 were apparent in anti-pS296 and -pS345 immunoprecipitates, respectively (Supplementary Figure S2A). These findings raised the new question of why only a few Chk1 molecules are phosphorylated simultaneously at Ser296 and ATR sites despite the fact that Ser296 phosphorylation depends on ATR-induced phosphorylation. One possible explanation is rapid dephosphorylation at ATR sites on Ser296-phosphorylated Chk1. In support of this model, we found that dephosphorylation at ATR sites was remarkably delayed in Chk1 mutated at Ser296 to Ala (S296A), compared with the WT case (Supplementary Figure S2B). In addition, treatment with UCN-01 (Supplementary Figure S2C) or protein phosphatase 2A (PP2A)-specific small-interfering RNA (siRNA) (Supplementary Figure S2D) attenuated the dephosphorylation reaction of ATR sites after the release of hydroxyurea. These observations are consistent with a previous report that PP2A promptly dephosphorylates ATR sites in a Chk1 kinase activity-dependent manner (Leung-Pineda *et al*, 2006). Thus, Ser296 phosphorylation, which occurs only on Chk1 phosphorylated at ATR sites, is likely to promote rapid dephosphorylation at ATR sites by protein phosphatases such as PP2A.

14-3-3γ directly binds Ser296-phosphorylated Chk1

To elucidate the functional changes of Chk1 because of Ser296 phosphorylation, we first measured the *in vitro* kinase activity of each Myc-Chk1 purified from UV-irradiated or non-treated cells. Between WT and S296A, we observed only marginal differences in the elevation of catalytic activity after UV irradiation (Figure 3A). Together with the previous findings for purified Chk1 protein (Chen *et al*, 2000), our observation suggested that Chk1 autophosphorylation exerts limited effects on catalytic activity.

We next searched for proteins binding to Chk1 in a Ser296 phosphorylation-dependent manner. As shown in Figure 3B, signals for anti-14-3-3γ (characterized in Supplementary Figure S3A) were detected in anti-Chk1 immunoprecipitates from UV-irradiated, but not non-treated cells. The signals were diminished by pre-treatment with UCN-01 (Figure 3B) or Chk1 mutations (S296A and K38M; Figure 3C). To further examine the relationship between Chk1 and 14-3-3, we performed the *in vitro* binding analyses using purified 14-3-3 proteins (Figure 3D) and GST-Chk1. As shown in Figure 3E, 14-3-3 bound to autophosphorylated Chk1 in a subtype-specific manner: γ had the highest affinity among all seven subtypes *in vitro*. GST pull-down assay from cell

